O modelowaniu zamarzania przechłodzonych kropelek wody w chmurach

S. Arabas[1], J.H. Curtis[2], A. Fridlind[3], D.A Knopf[4], M. West[2] & N. Riemer[2]

1: agh.edu.pl
2: atmos.illinois.edu
3: giss.nasa.gov
4: stonybrook.edu

finansowanie:
ASR Atmospheric System Research
NCN POLAND

Seminarium Wydziału Fizyki i Informatyki Stosowanej AGH, 26.V 2023 r.

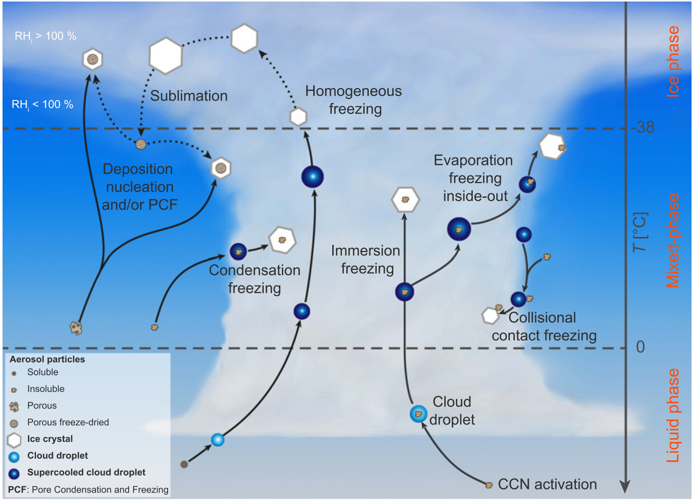

Kanji et al. 2017, graphics F. Mahrt, `https://doi.org/10.1175/AMSMONOGRAPHS-D-16-0006.1`

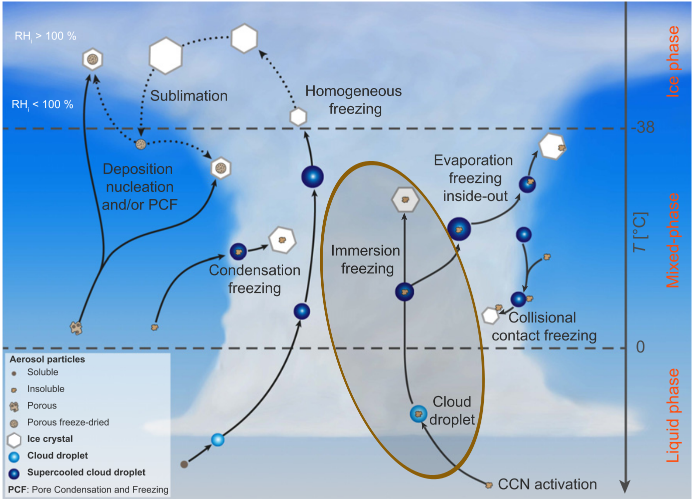

Kanji et al. 2017, graphics F. Mahrt, https://doi.org/10.1175/AMSMONOGRAPHS-D-16-0006.1

https://www.reuters.com/markets/commodities/making-snow-stick-wind-challenges-winter-games-slope-makers-2021-11-29/

https://www.reuters.com/markets/commodities/making-snow-stick-wind-challenges-winter-games-slope-makers-2021-11-29/

Journal of Geophysical Research: Atmospheres

RESEARCH ARTICLE

10.1002/2016JD025251

The unstable ice nucleation properties of Snomax® bacterial particles

Michael Polen[1], Emily Lawlis[1], and Ryan C. Sullivan[1]

[1]Center for Atmospheric Particle Studies, Carnegie Mellon University, Pittsburgh, Pennsylvania, USA

Key Points:
- Very ice active Snomax protein aggregates are fragile and their ice nucleation ability decreases over months of freezer storage
- Partitioning of ice active protein aggregates into the immersion oil reduces the droplet's measured freezing temperature
- Caution is warranted in the use of

Abstract Snomax® is often used as a surrogate for biological ice nucleating particles (INPs) and has recently been proposed as an INP standard for evaluating ice nucleation methods. We have found the immersion freezing properties of Snomax particles to be substantially unstable, observing a loss of ice nucleation ability

WIKIPEDIA
The Free Encyclopedia

Cat's Cradle

Cat's Cradle is a satirical postmodern novel, with science fiction elements, by American writer Kurt Vonnegut. Vonnegut's fourth novel, it was first published in 1963, exploring and satirizing issues of science, technology, the purpose of religion, and the arms race, often through the use of morbid humor.

Cat's Cradle

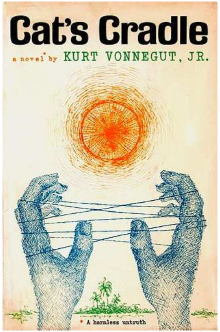

First edition hardback cover

Author	Kurt Vonnegut
Original title	*Cat's Cradle*
Country	United States
Language	English

Synopsis

Background

The first-person everyman narrator, a professional writer introducing himself as Jonah (but apparently named John and never named again), frames the plot as a flashback. Set in the mid-20th century, the plot revolves around a time when he was planning to write a book called *The Day the World Ended* about what people were doing on the day of the atomic bombing of Hiroshima. Throughout, he also intersperses meaningful as well as sarcastic passages and sentiments from an odd religious scripture known as *The Books of Bokonon*. The events of the novel evidently occur before the narrator was converted to his current religion, Bokononism.

Plot summary

While researching for his upcoming book, the narrator travels to Ilium, New York, the hometown of the late Felix Hoenikker, a co-creator of the atomic bomb and Nobel laureate physicist, to interview Hoenikker's children, coworkers, and other acquaintances. There, he learns of a substance called *ice-nine*, created for military use by Hoenikker and now likely in the possession of his three adult children. *Ice-nine* is an alternative structure of water that is solid at room temperature and acts as a seed crystal upon contact with ordinary liquid water, causing that liquid water to instantly freeze and transform into more *ice-nine*. Among

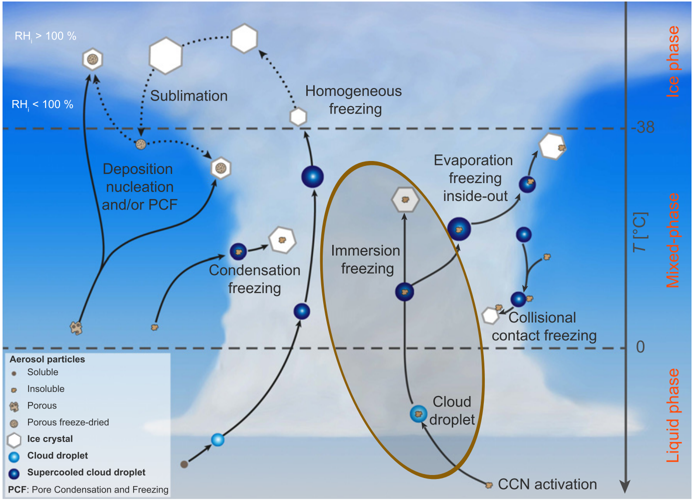

Kanji et al. 2017, graphics F. Mahrt, https://doi.org/10.1175/AMSMONOGRAPHS-D-16-0006.1

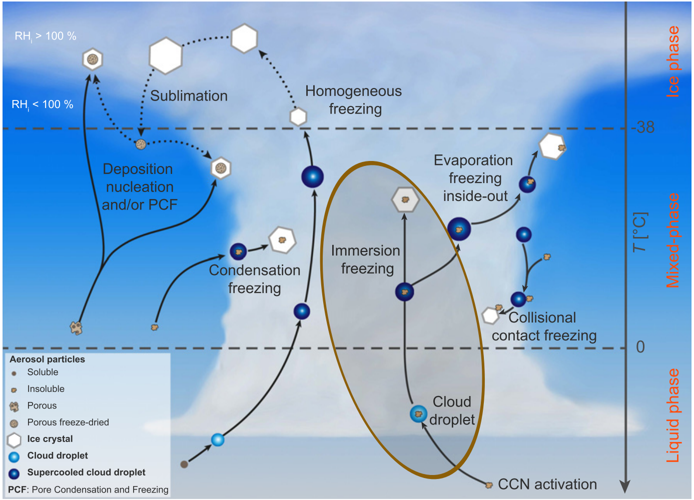

Kanji et al. 2017, graphics F. Mahrt, https://doi.org/10.1175/AMSMONOGRAPHS-D-16-0006.1

Vonnegut 1948 (J. Colloid Sci.)

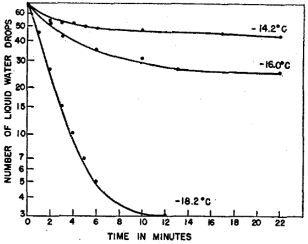

Fraction of water drops remaining unfrozen as a function of time.

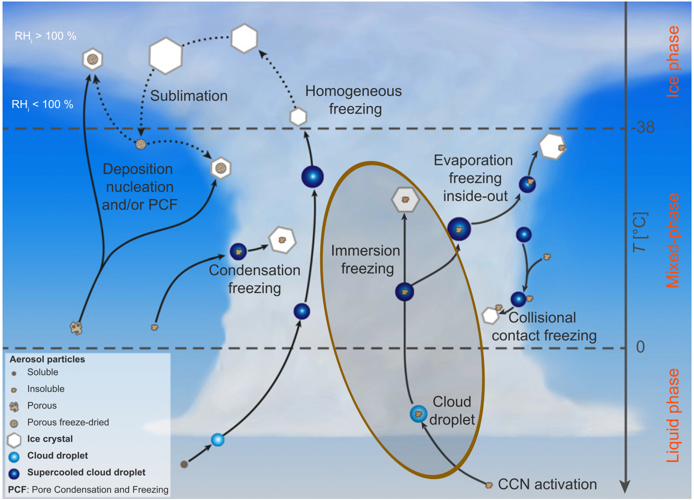

Kanji et al. 2017, graphics F. Mahrt, https://doi.org/10.1175/AMSMONOGRAPHS-D-16-0006.1

Vonnegut 1948 (J. Colloid Sci.)

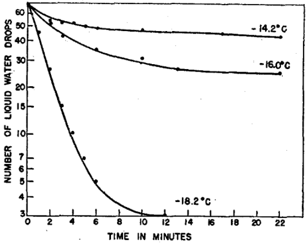

Fraction of water drops remaining unfrozen as a function of time.

Vali 2014 (ACP)

"Interpretations of the experimental results face considerable difficulties ... two separate ways of interpreting the same observations; one assigned primacy to time the other emphasized the temperature-dependent impacts of the impurities ... dichotomy – the stochastic and singular models"

Heterogeneous Nucleations is a Stochastic Process

by

J. S. MARSHALL

McGill University, Montreal, Canad.

Presented at the International Congress on the Physics of Clouds (Hailstorms) at Verona 9-13 August 1960.

http://cma.entecra.it/Astro2_sito/doc/Nubila_1_1961.pdf

theory (in modern notation)
(Bigg '53, Langham & Mason '58, Carte '59, Marshall '61)

theory (in modern notation)
(Bigg '53, Langham & Mason '58, Carte '59, Marshall '61)

Poisson counting process with rate r:

$$P^*(\text{k events in time t}) = \frac{(rt)^k \exp(-rt)}{k!}$$

$$P(\text{one or more events in time t}) = 1 - P^*(k = 0, t)$$

$$\ln(1 - P) = -rt$$

theory (in modern notation)

(Bigg '53, Langham & Mason '58, Carte '59, Marshall '61)

Poisson counting process with rate r:

$$P^*(\text{k events in time t}) = \frac{(rt)^k \exp(-rt)}{k!}$$

$$P(\text{one or more events in time t}) = 1 - P^*(k=0, t)$$

$$\ln(1-P) = -rt$$

introducing $J_{\text{het}}(T)$, $T(t)$ and INP surface A:

$$\ln\left(1-P(A,t)\right) = -A\underbrace{\int_0^t J_{\text{het}}(T(t'))\,dt'}_{n_s(T)}$$

theory (in modern notation)
(Bigg '53, Langham & Mason '58, Carte '59, Marshall '61)

Poisson counting process with rate r:

$$P^*(\text{k events in time t}) = \frac{(rt)^k \exp(-rt)}{k!}$$

$$P(\text{one or more events in time t}) = 1 - P^*(k=0, t)$$

$$\ln(1-P) = -rt$$

introducing $J_{het}(T)$, $T(t)$ and INP surface A:

$$\ln\left(1 - P(A,t)\right) = -A \underbrace{\int_0^t J_{het}(T(t'))\, dt'}_{n_s(T)}$$

experimental fits (same data, both exp-linear):

INAS (Niemand et al.): $n_s(T) = \dots$

theory (in modern notation)
(Bigg '53, Langham & Mason '58, Carte '59, Marshall '61)

Poisson counting process with rate r:

$$P^*(\text{k events in time t}) = \frac{(rt)^k \exp(-rt)}{k!}$$

$$P(\text{one or more events in time t}) = 1 - P^*(k=0, t)$$

$$\ln(1-P) = -rt$$

introducing $J_{\text{het}}(T)$, $T(t)$ and INP surface A:

$$\ln(1-P(A,t)) = -A\underbrace{\int_0^t J_{\text{het}}(T(t'))\,dt'}_{n_s(T)}$$

experimental fits (same data, both exp-linear):

INAS (Niemand et al.): $n_s(T) = \ldots$

CNT/ABIFM (Knopf et al.): $J_{\text{het}}(a_w(T)) = \ldots$

a_w – water activity

AIDA @ KIT

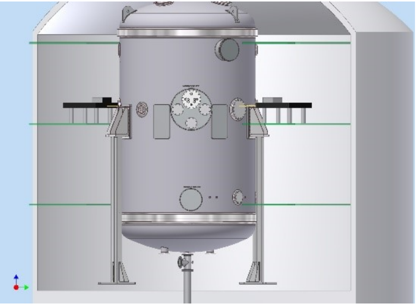  

(https://www.imk-aaf.kit.edu/73.php, photo: KIT/Ottmar Möhler)

particle attribute sampling

random sampling of immersed surface for each particle

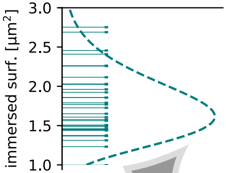

random sampling of freezing temperatures
(conditional distribution for a given surface)

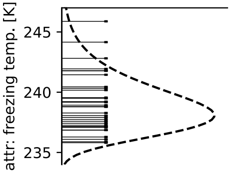

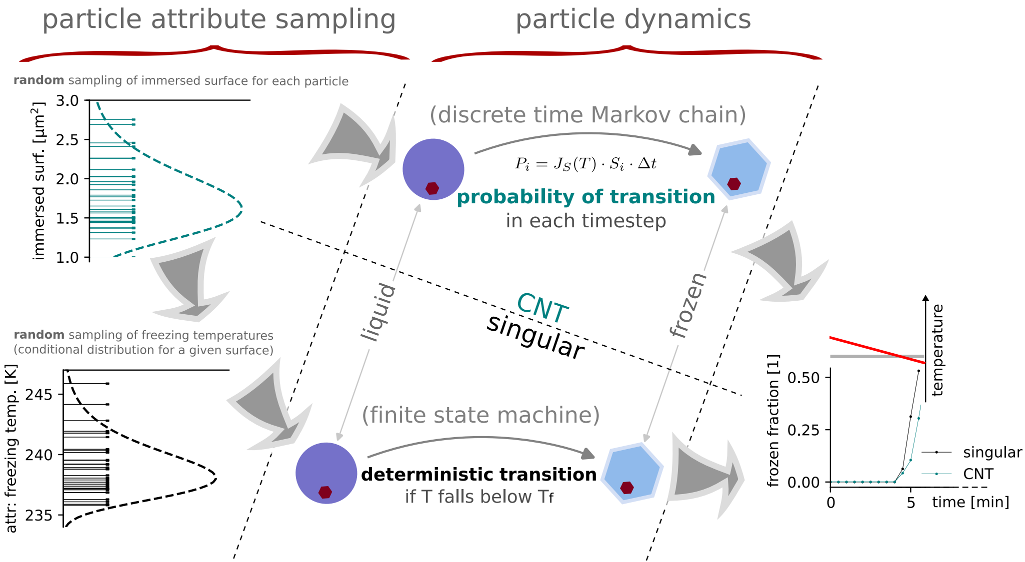

particle attribute sampling
particle dynamics
random sampling of immersed surface for each particle
immersed surf. [μm²]
3.0
2.5
2.0
1.5
1.0
random sampling of freezing temperatures
(conditional distribution for a given surface)
attr: freezing temp. [K]
245
240
235
(discrete time Markov chain)
$P_i = J_S(T) \cdot S_i \cdot \Delta t$
probability of transition
in each timestep
liquid
frozen
CNT
singular
(finite state machine)
deterministic transition
if T falls below Tf
frozen fraction [1]
0.50
0.25
0.00
0
5
time [min]
temperature
singular
CNT

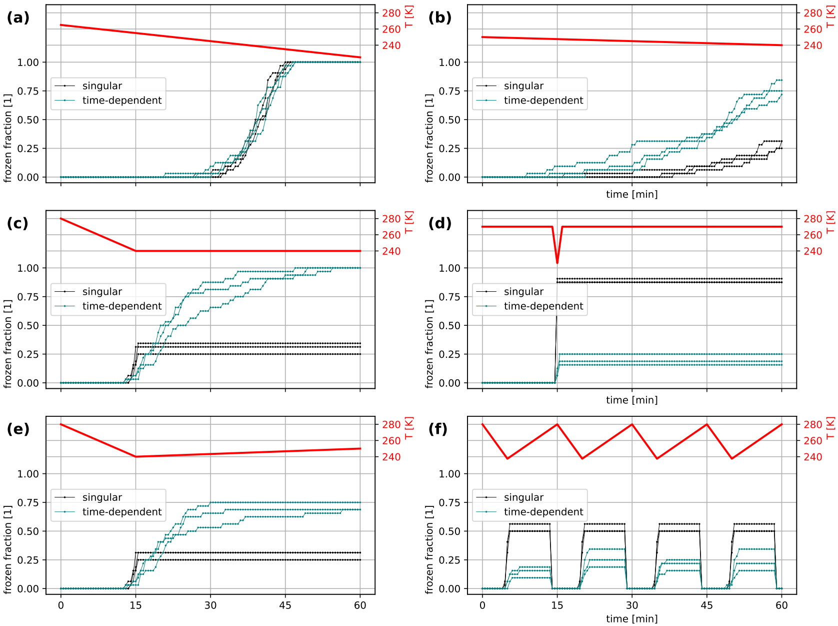

(a)
(b)
(c)
(d)
(e)
(f)
280
260
240
T [K]
1.00
0.75
0.50
0.25
0.00
frozen fraction [1]
singular
time-dependent
0
15
30
45
60
time [min]

AIDA @ KIT

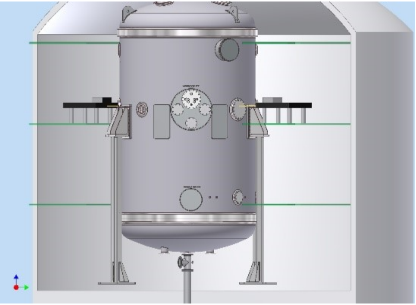  

(https://www.imk-aaf.kit.edu/73.php, photo: KIT/Ottmar Möhler)

AIDA cooling rate: $0.5\,{}^{K}/_{min}$

theory (in modern notation)
(Bigg '53, Langham & Mason '58, Carte '59, Marshall '61)

Poisson counting process with rate r:

$$P^*(\text{k events in time t}) = \frac{(rt)^k \exp(-rt)}{k!}$$

$$P(\text{one or more events in time t}) = 1 - P^*(k=0,t)$$

$$\ln(1-P) = -rt$$

introducing $J_{\text{het}}(T)$, $T(t)$ and INP surface A:

$$\ln\left(1 - P(A,t)\right) = -A \underbrace{\int_0^t J_{\text{het}}(T(t'))\, dt'}_{n_s(T)}$$

experimental fits (same data, both exp-linear):

INAS (Niemand et al.): $n_s(T) = \ldots$

CNT/ABIFM (Knopf et al.): $J_{\text{het}}(a_w(T)) = \ldots$

a_w – water activity

theory (in modern notation)
(Bigg '53, Langham & Mason '58, Carte '59, Marshall '61)

Poisson counting process with rate r:

$$P^*(\text{k events in time t}) = \frac{(rt)^k \exp(-rt)}{k!}$$

$$P(\text{one or more events in time t}) = 1 - P^*(k=0, t)$$

$$\ln(1-P) = -rt$$

introducing $J_{\text{het}}(T)$, $T(t)$ and INP surface A:

$$\ln(1-P(A,t)) = \underbrace{-A\int_0^t J_{\text{het}}(T(t'))\,dt'}_{n_s(T)}$$

experimental fits (same data, both exp-linear):

INAS (Niemand et al.): $n_s(T) = \ldots$

CNT/ABIFM (Knopf et al.): $J_{\text{het}}(a_w(T)) = \ldots$

a_w – water activity

for a constant cooling rate $c = dT/dt$:

$$\ln(1-P(A,t)) = -\frac{A}{c}\int_{T_0}^{T_0+ct} J_{\text{het}}(T')dT' = -A \cdot n_s(T)$$

theory (in modern notation)
(Bigg '53, Langham & Mason '58, Carte '59, Marshall '61)

Poisson counting process with rate r:

$$P^*(\text{k events in time t}) = \frac{(rt)^k \exp(-rt)}{k!}$$

$$P(\text{one or more events in time t}) = 1 - P^*(k=0,t)$$

$$\ln(1-P) = -rt$$

introducing $J_{\text{het}}(T)$, $T(t)$ and INP surface A:

$$\ln(1-P(A,t)) = \underbrace{-A\int_0^t J_{\text{het}}(T(t'))\,dt'}_{n_s(T)}$$

experimental fits (same data, both exp-linear):

INAS (Niemand et al.): $n_s(T) = \ldots$

CNT/ABIFM (Knopf et al.): $J_{\text{het}}(a_w(T)) = \ldots$

a_w – water activity

for a constant cooling rate $c = dT/dt$:

$$\ln(1-P(A,t)) = -\frac{A}{c}\int_{T_0}^{T_0+ct} J_{\text{het}}(T')dT' = -A \cdot n_s(T)$$

$$\frac{dn_s(T)}{dT} = a \cdot n_s(T) = -\frac{1}{c}J_{\text{het}}(T)$$

theory (in modern notation)
(Bigg '53, Langham & Mason '58, Carte '59, Marshall '61)

Poisson counting process with rate r:

$$P^*(\text{k events in time t}) = \frac{(rt)^k \exp(-rt)}{k!}$$

$$P(\text{one or more events in time t}) = 1 - P^*(k=0, t)$$

$$\ln(1-P) = -rt$$

introducing $J_{\text{het}}(T)$, $T(t)$ and INP surface A:

$$\ln\left(1-P(A,t)\right) = -A\underbrace{\int_0^t J_{\text{het}}(T(t'))\,dt'}_{n_s(T)}$$

experimental fits (same data, both exp-linear):

INAS (Niemand et al.): $n_s(T) = \ldots$

CNT/ABIFM (Knopf et al.): $J_{\text{het}}(a_w(T)) = \ldots$

a_w – water activity

for a constant cooling rate $c = dT/dt$:

$$\ln(1-P(A,t)) = -\frac{A}{c}\int_{T_0}^{T_0+ct} J_{\text{het}}(T')dT' = -A \cdot n_s(T)$$

$$\frac{dn_s(T)}{dT} = a \cdot n_s(T) = -\frac{1}{c}J_{\text{het}}(T)$$

experimental fits

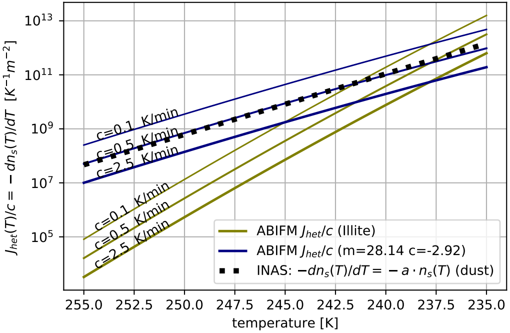

problem ?!

for a constant cooling rate $c = dT/dt$:

$$\ln(1 - P(A,t)) = -\frac{A}{c}\int_{T_0}^{T_0+ct} J_{\mathrm{het}}(T')dT' = -A \cdot n_s(T)$$

$$\frac{dn_s(T)}{dT} = a \cdot n_s(T) = -\frac{1}{c} J_{\mathrm{het}}(T)$$

experimental fits

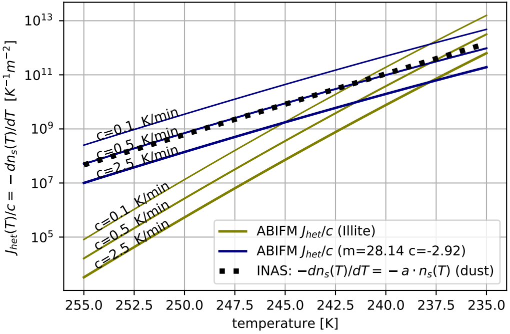

Shima, Sato, Hashimoto & Misumi 2020 (GMD):

Predicting the morphology of ice particles in deep convection using the super-droplet method

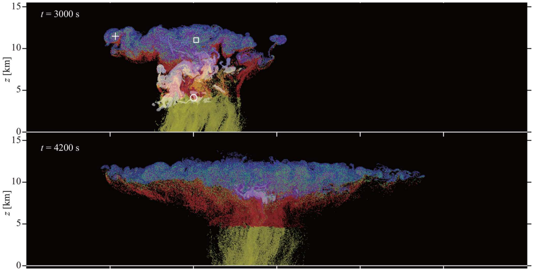

Figure 1. Typical realization of CTRL cloud spatial structures at $t = 2040$, 2460, 3000, 4200, and 5400 s. The mixing ratio of cloud water, rainwater, cloud ice, graupel, and snow aggregates are plotted in fading white, yellow, blue, red, and green, respectively. The symbols indicate examples of unrealistic predicted ice particles (Sects. 7.3 and 9.1). See also Movie 1 in the video supplement.

Shima, Sato, Hashimoto & Misumi 2020 (GMD):

Predicting the morphology of ice particles in deep convection using the super-droplet method

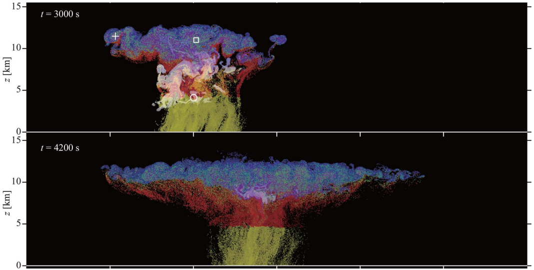

Figure 1. Typical realization of CTRL cloud spatial structures at $t = 2040$, 2460, 3000, 4200, and 5400 s. The mixing ratio of cloud water, rainwater, cloud ice, graupel, and snow aggregates are plotted in fading white, yellow, blue, red, and green, respectively. The symbols indicate examples of unrealistic predicted ice particles (Sects. 7.3 and 9.1). See also Movie 1 in the video supplement.

- Eulerian component: momentum, heat, moisture budget

Shima, Sato, Hashimoto & Misumi 2020 (GMD):
Predicting the morphology of ice particles in deep convection using the super-droplet method

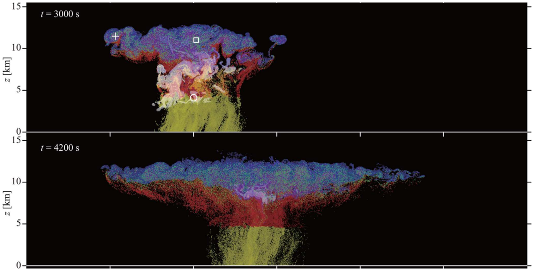

Figure 1. Typical realization of CTRL cloud spatial structures at $t = 2040$, 2460, 3000, 4200, and 5400 s. The mixing ratio of cloud water, rainwater, cloud ice, graupel, and snow aggregates are plotted in fading white, yellow, blue, red, and green, respectively. The symbols indicate examples of unrealistic predicted ice particles (Sects. 7.3 and 9.1). See also Movie 1 in the video supplement.

- Eulerian component: momentum, heat, moisture budget
- Lagrangian component: super particles representing aerosol, water droplets, ice particles (porous spheroids)

Shima, Sato, Hashimoto & Misumi 2020 (GMD):

Predicting the morphology of ice particles in deep convection using the super-droplet method

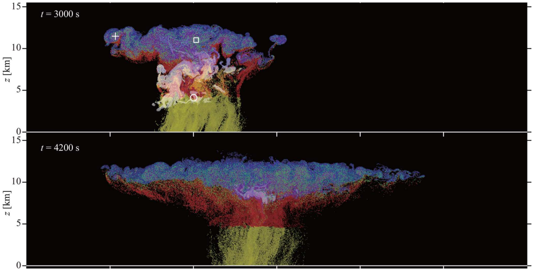

Figure 1. Typical realization of CTRL cloud spatial structures at $t = 2040$, 2460, 3000, 4200, and 5400 s. The mixing ratio of cloud water, rainwater, cloud ice, graupel, and snow aggregates are plotted in fading white, yellow, blue, red, and green, respectively. The symbols indicate examples of unrealistic predicted ice particles (Sects. 7.3 and 9.1). See also Movie 1 in the video supplement.

- Eulerian component: momentum, heat, moisture budget
- Lagrangian component: super particles representing aerosol, water droplets, ice particles (porous spheroids)

- particle-resolved processes:
  — advection and sedimentation
  — homogeneous and immersion freezing (singular)
  — melting
  — condensation and evaporation (incl. CCN [de]activation)
  — deposition and sublimation
  — collisions (coalescence, riming, aggregation, washout)

Shima, Sato, Hashimoto & Misumi 2020 (GMD):

Predicting the morphology of ice particles in deep convection using the super-droplet method

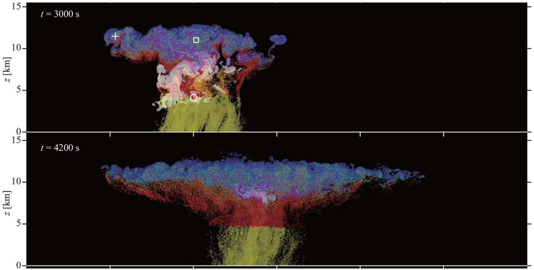

Figure 1. Typical realization of CTRL cloud spatial structures at $t = 2040$, 2460, 3000, 4200, and 5400 s. The mixing ratio of cloud water, rainwater, cloud ice, graupel, and snow aggregates are plotted in fading white, yellow, blue, red, and green, respectively. The symbols indicate examples of unrealistic predicted ice particles (Sects. 7.3 and 9.1). See also Movie 1 in the video supplement.

- Eulerian component: momentum, heat, moisture budget
- Lagrangian component: super particles representing aerosol, water droplets, ice particles (porous spheroids)

- particle-resolved processes:
  — advection and sedimentation
  — homogeneous and immersion freezing (singular)
  — melting
  — condensation and evaporation (incl. CCN [de]activation)
  — deposition and sublimation
  — collisions (coalescence, riming, aggregation, washout)

- 2D Cb test case

Shima, Sato, Hashimoto & Misumi 2020 (GMD): *Predicting the morphology of ice particles in deep convection using the super-droplet method*

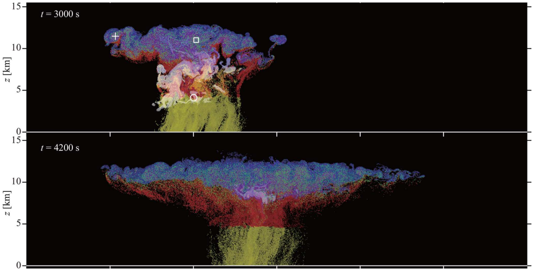

Figure 1. Typical realization of CTRL cloud spatial structures at $t = 2040$, 2460, 3000, 4200, and 5400 s. The mixing ratio of cloud water, rainwater, cloud ice, graupel, and snow aggregates are plotted in fading white, yellow, blue, red, and green, respectively. The symbols indicate examples of unrealistic predicted ice particles (Sects. 7.3 and 9.1). See also Movie 1 in the video supplement.

- Eulerian component: momentum, heat, moisture budget
- Lagrangian component: super particles representing aerosol, water droplets, ice particles (porous spheroids)
- particle-resolved processes:
  — advection and sedimentation
  — homogeneous and immersion freezing (singular)
  — melting
  — condensation and evaporation (incl. CCN [de]activation)
  — deposition and sublimation
  — collisions (coalescence, riming, aggregation, washout)
- 2D Cb test case

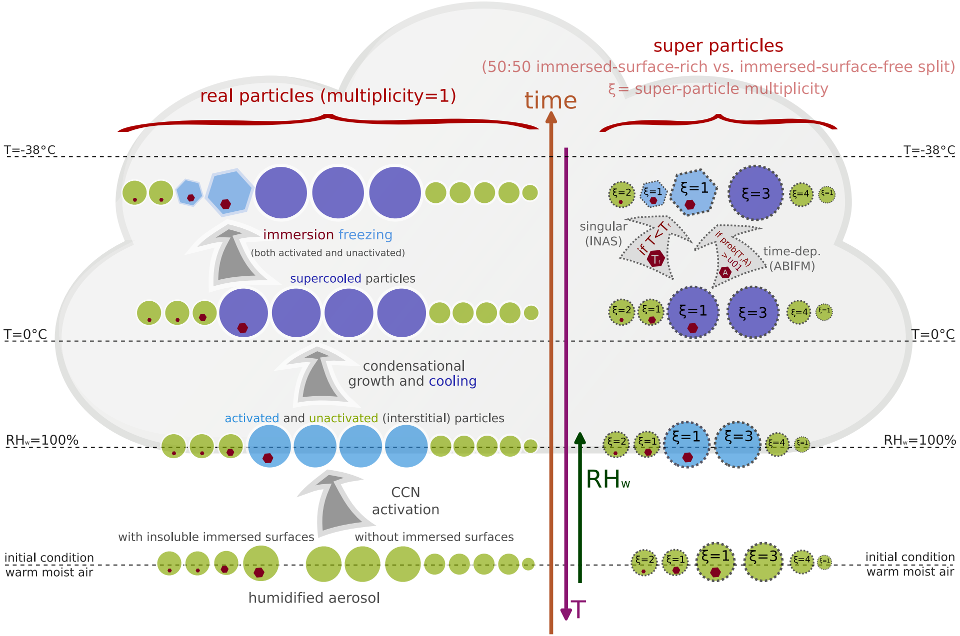
super particles
(50:50 immersed-surface-rich vs. immersed-surface-free split)
ξ = super-particle multiplicity
real particles (multiplicity=1)
time
T=-38°C
T=-38°C
immersion freezing
(both activated and unactivated)
singular (INAS)
time-dep. (ABIFM)
supercooled particles
T=0°C
T=0°C
condensational growth and cooling
activated and unactivated (interstitial) particles
RHw=100%
RHw=100%
RHw
CCN activation
with insoluble immersed surfaces
without immersed surfaces
initial condition warm moist air
initial condition warm moist air
humidified aerosol
T

new open-source HPC packages: Bartman et al. 2022 (JOSS)

new open-source HPC packages: Bartman et al. 2022 (JOSS)


Search projects

Help Sponsors Log in Register

PySDM 2.20

`pip install PySDM`

Latest version

Released: Apr 21, 2023

Pythonic particle-based (super-droplet) warm-rain/aqueous-chemistry cloud microphysics package with box, parcel & 1D/2D prescribed-flow examples in Python, Julia and Matlab

Navigation

Project description

Release history

Download files

Project links

Homepage

Documentation

Source

Tracker

Statistics

GitHub statistics:

Stars: 40

Forks: 21

Open issues: 101

Open PRs: 13

Project description

PySDM

License GPL v3

tests+artifacts+pypi passing | build passing | codecov 78%

pypi package 2.20 | API docs pdoc3

PySDM is a package for simulating the dynamics of population of particles. It is intended to serve as a building block for simulation systems modelling fluid flows involving a dispersed phase, with PySDM being responsible for representation of the dispersed phase. Currently, the development is focused on atmospheric cloud physics applications, in particular on modelling the dynamics of particles immersed in moist air using the particle-based (a.k.a. super-droplet) approach to represent aerosol/cloud/rain microphysics. The package features a Pythonic high-performance implementation of the Super-Droplet Method (SDM) Monte-Carlo algorithm for representing collisional growth (Shima et al. 2009), hence the name.

PySDM has two alternative parallel number-crunching backends available: multi-threaded CPU backend based on Numba and GPU-resident backend built on top of ThrustRTC. The `Numba` backend (aliased `CPU`) features multi-threaded parallelism for multi-core CPUs, it uses the just-in-time compilation technique based on the LLVM infrastructure. The `ThrustRTC` backend (aliased `GPU`) offers


Search projects

Help Sponsors Log in Register

PyMPDATA 1.0.11

`pip install PyMPDATA`

Latest version

Released: Apr 26, 2023

Numba-accelerated Pythonic implementation of MPDATA with examples in Python, Julia and Matlab

Navigation

Project description

Release history

Download files

Project links

Documentation

Source

Tracker

Statistics

GitHub statistics:

Stars: 19

Forks: 10

Open issues: 25

Open PRs: 3

View statistics for this project via Libraries.io,

Project description

PyMPDATA

tests+pypi passing | build passing | codecov 92%

pypi package 1.0.11 | API docs pdoc3

PyMPDATA is a high-performance Numba-accelerated Pythonic implementation of the MPDATA algorithm of Smolarkiewicz et al. used in geophysical fluid dynamics and beyond. MPDATA numerically solves generalised transport equations - partial differential equations used to model conservation/balance laws, scalar-transport problems, convection-diffusion phenomena. As of the current version, PyMPDATA supports homogeneous transport in 1D, 2D and 3D using structured meshes, optionally generalised by employment of a Jacobian of coordinate transformation. PyMPDATA includes implementation of a set of MPDATA variants including the non-oscillatory option, infinite-gauge, divergent-flow, double-pass donor cell (DPDC) and third-order-terms options. It also features support for integration of Fickian-terms in advection-diffusion problems using the pseudo-transport velocity approach. In 2D and 3D simulations, domain-decomposition is used for multi-threaded parallelism.

PyMPDATA is engineered purely in Python targeting both performance and usability, the latter encompassing research users', developers' and maintainers' perspectives. From researcher's perspective, PyMPDATA offers hassle-free

JAGIELLONIAN UNIVERSITY IN KRAKÓW

Caltech

ILLINOIS

new open-source HPC packages: Bartman et al. 2022 (JOSS)

JAGIELLONIAN UNIVERSITY IN KRAKÓW Caltech ILLINOIS

maintanance & development ⇝ AGH: SA, Oleksii Bulenok, Kacper Derlatka

Lagrangian component (PySDM)

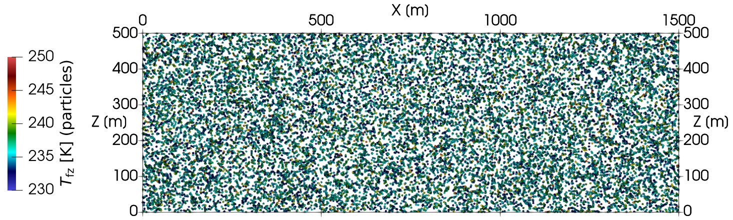

Eulerian component (PyMPDATA)

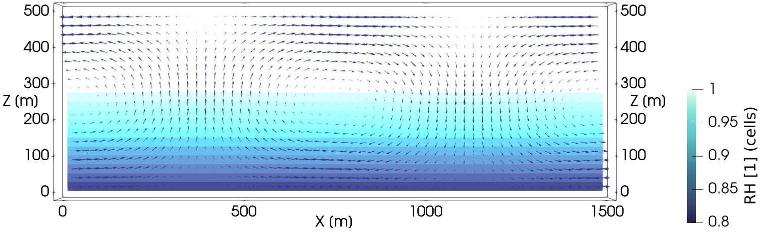

$w_{max} \approx 1/3$ m/s

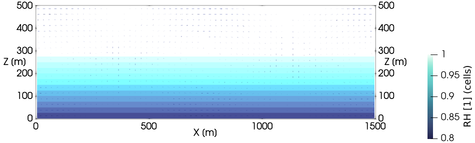

$w_{max} \approx 1$ m/s

$w_{max} \approx 3$ m/s

$w_{max} \approx 1/3$ m/s

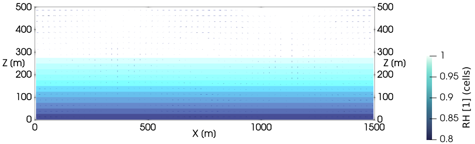

$w_{max} \approx 1$ m/s

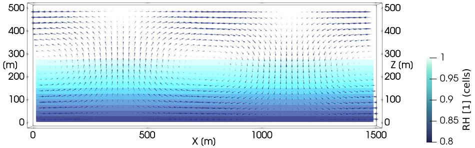

$w_{max} \approx 3$ m/s

$w_{max} \approx 1/3$ m/s

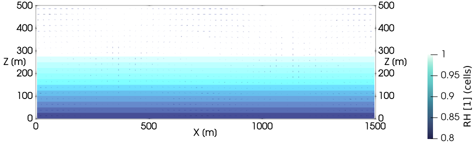

$w_{max} \approx 1$ m/s

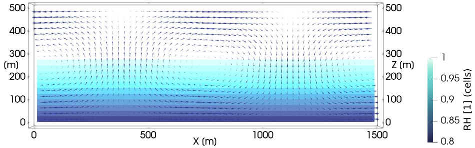

$w_{max} \approx 3$ m/s

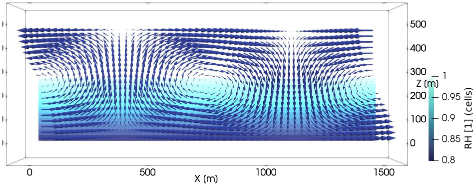

$w_{max} \approx 1/3$ m/s

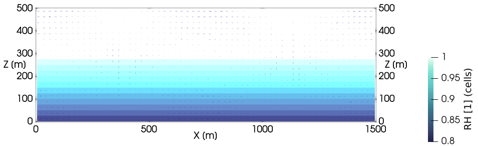

$w_{max} \approx 1$ m/s

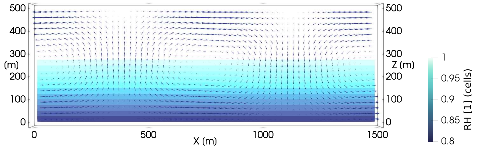

$w_{max} \approx 3$ m/s

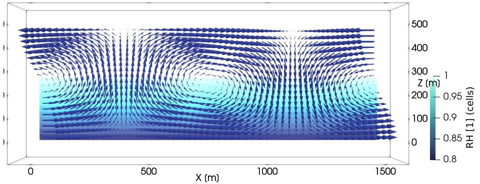

singular (INAS)

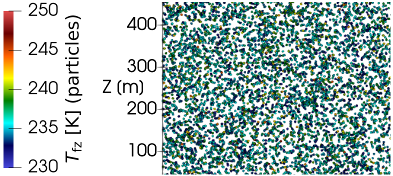

time-dependent (J_{het})

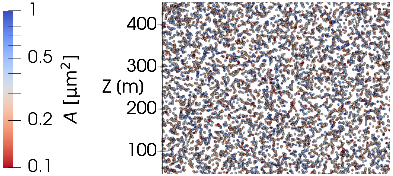

Time: 30 s (spin-up till 600.0 s)

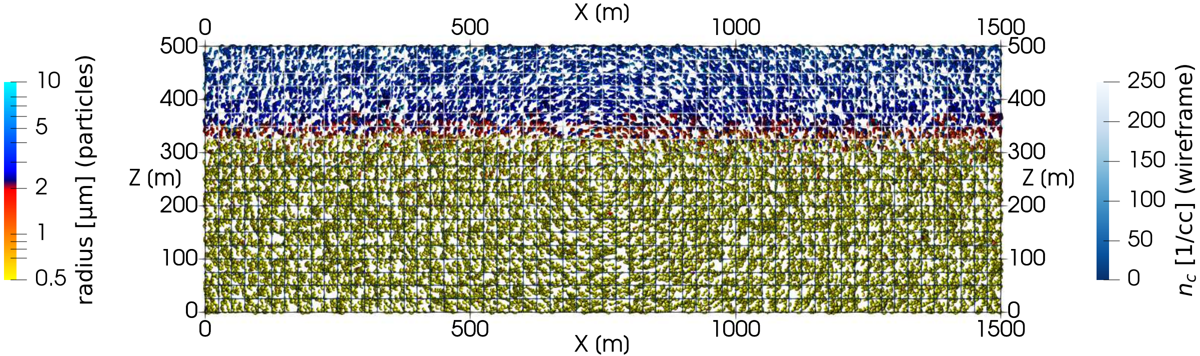

16+16 super-particles/cell for INP-rich + INP-free particles

$N_{aer} = 300/cc$ (two-mode lognormal) $N_{INP} = 150/L$ (lognormal, $D_g = 0.74$ µm, $\sigma_g = 2.55$)

spin-up = freezing off; subsequently frozen particles act as tracers

Time: 60 s (spin-up till 600.0 s)

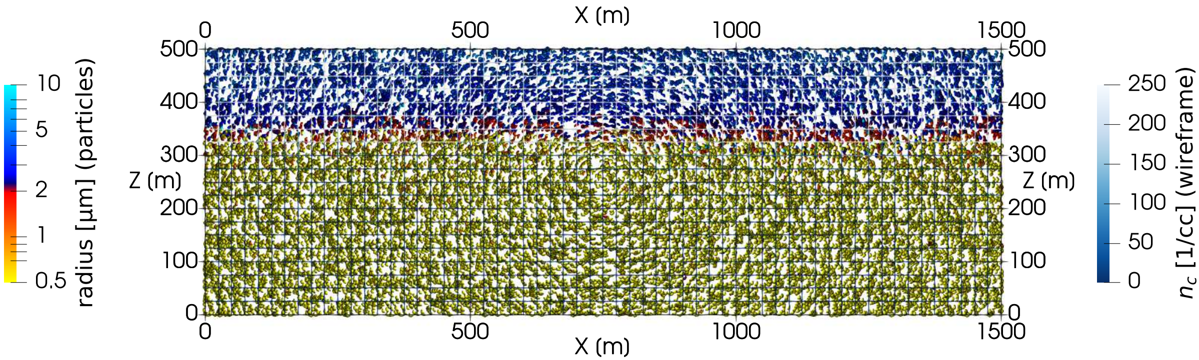

16+16 super-particles/cell for INP-rich + INP-free particles

$N_{\text{aer}} = 300/cc$ (two-mode lognormal) $N_{\text{INP}} = 150/L$ (lognormal, $D_g = 0.74$ µm, $\sigma_g = 2.55$)

spin-up = freezing off; subsequently frozen particles act as tracers

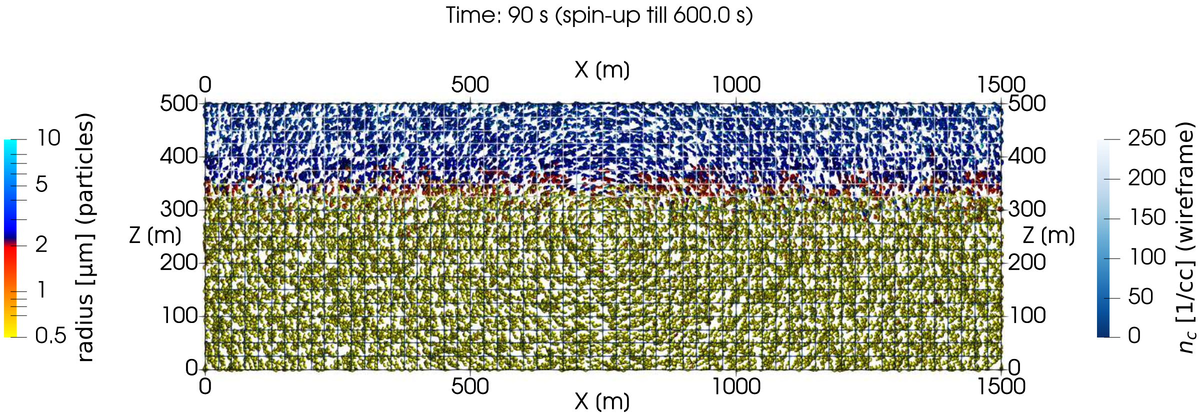

16+16 super-particles/cell for INP-rich + INP-free particles
$N_{aer} = 300/cc$ (two-mode lognormal) $N_{INP} = 150/L$ (lognormal, $D_g = 0.74$ μm, $\sigma_g = 2.55$)
spin-up = freezing off; subsequently frozen particles act as tracers

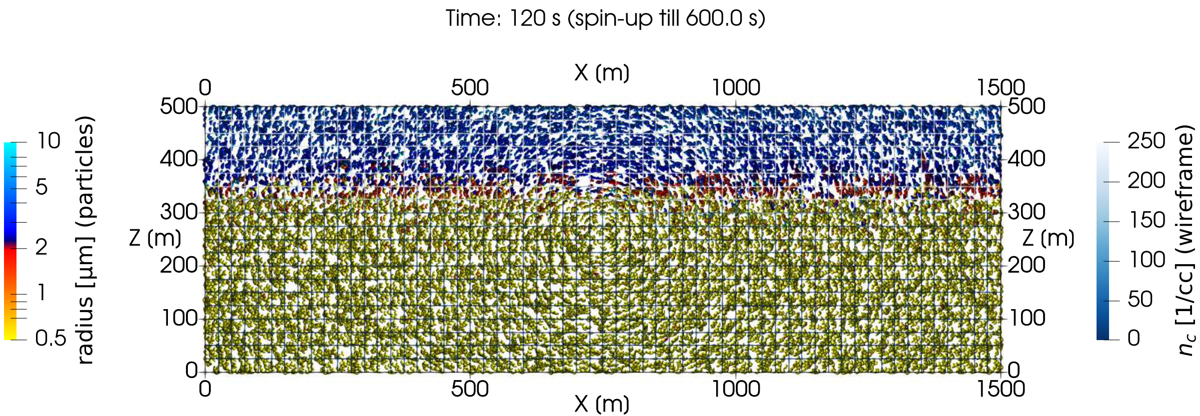

16+16 super-particles/cell for INP-rich + INP-free particles
$N_{aer} = 300/cc$ (two-mode lognormal) $N_{INP} = 150/L$ (lognormal, $D_g = 0.74$ μm, $\sigma_g = 2.55$)
spin-up = freezing off; subsequently frozen particles act as tracers

Time: 150 s (spin-up till 600.0 s)

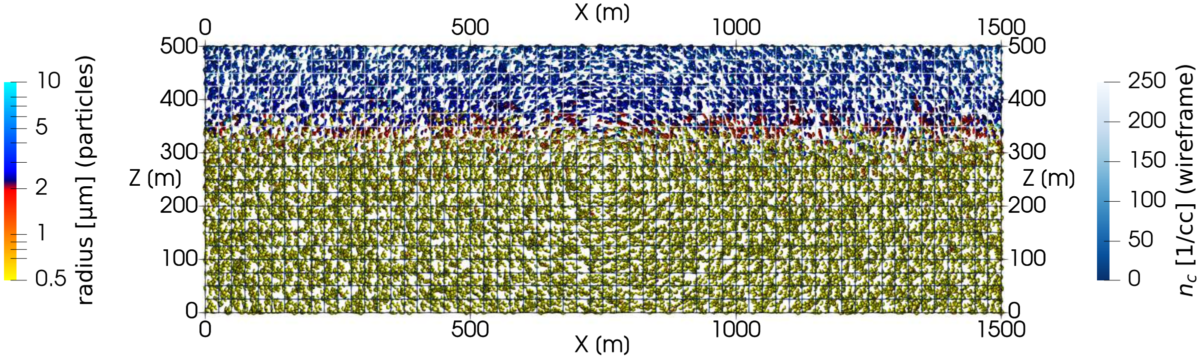

16+16 super-particles/cell for INP-rich + INP-free particles

$N_{aer} = 300/cc$ (two-mode lognormal) $N_{INP} = 150/L$ (lognormal, $D_g = 0.74$ μm, $\sigma_g = 2.55$)

spin-up = freezing off; subsequently frozen particles act as tracers

Time: 180 s (spin-up till 600.0 s)

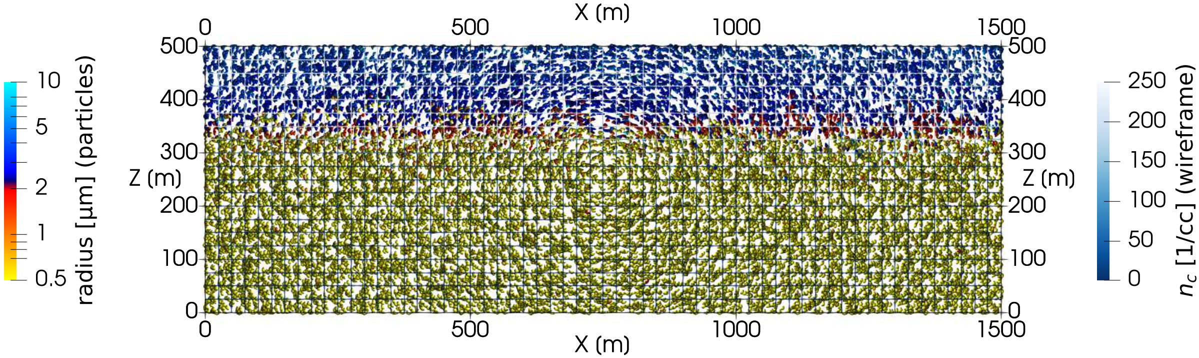

16+16 super-particles/cell for INP-rich + INP-free particles

$N_{\text{aer}} = 300/cc$ (two-mode lognormal) $N_{\text{INP}} = 150/L$ (lognormal, $D_g = 0.74$ μm, $\sigma_g = 2.55$)

spin-up = freezing off; subsequently frozen particles act as tracers

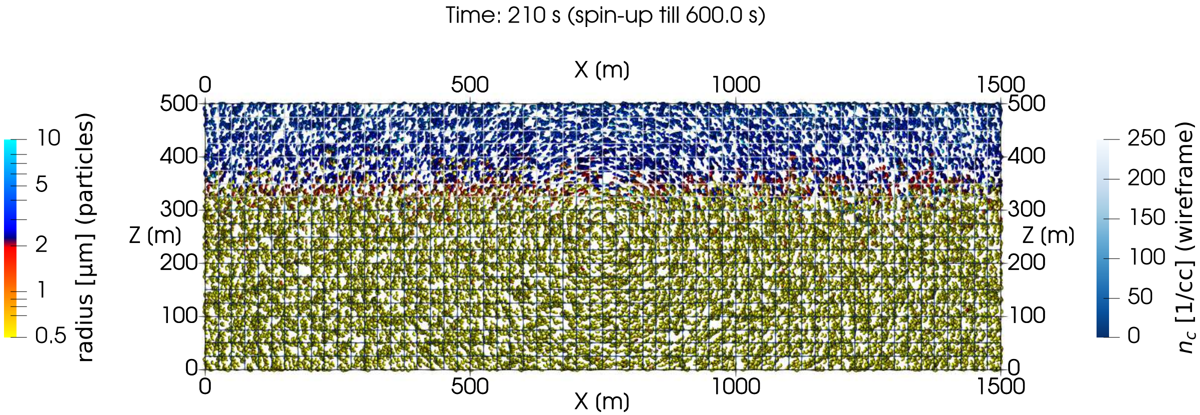

16+16 super-particles/cell for INP-rich + INP-free particles

$N_{aer} = 300/cc$ (two-mode lognormal) $N_{INP} = 150/L$ (lognormal, $D_g = 0.74$ µm, $\sigma_g = 2.55$)

spin-up = freezing off; subsequently frozen particles act as tracers

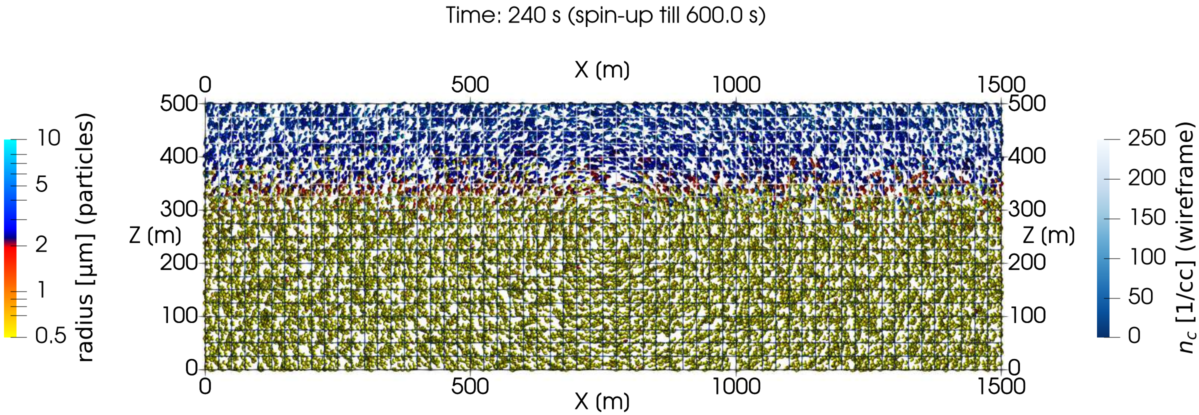

16+16 super-particles/cell for INP-rich + INP-free particles

$N_{aer} = 300/cc$ (two-mode lognormal) $N_{INP} = 150/L$ (lognormal, $D_g = 0.74$ µm, $\sigma_g = 2.55$)

spin-up = freezing off; subsequently frozen particles act as tracers

Time: 270 s (spin-up till 600.0 s)

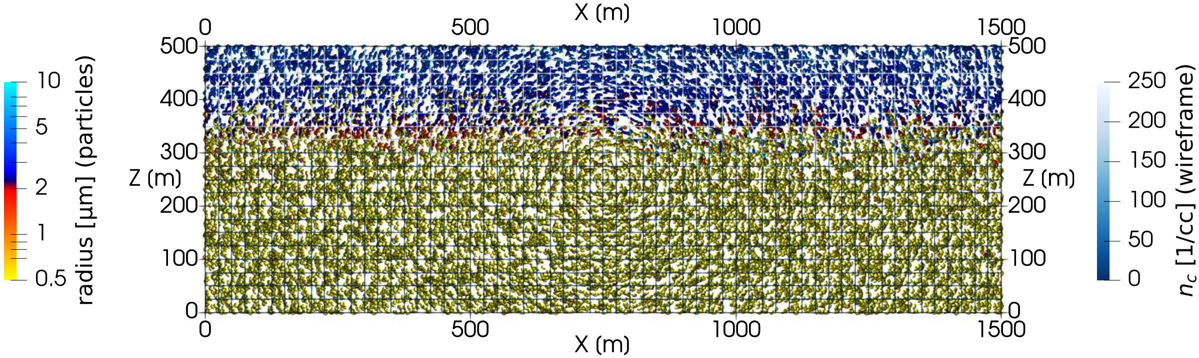

16+16 super-particles/cell for INP-rich + INP-free particles

$N_{\text{aer}} = 300/cc$ (two-mode lognormal) $N_{\text{INP}} = 150/L$ (lognormal, $D_g = 0.74$ μm, $\sigma_g = 2.55$)

spin-up = freezing off; subsequently frozen particles act as tracers

Time: 300 s (spin-up till 600.0 s)

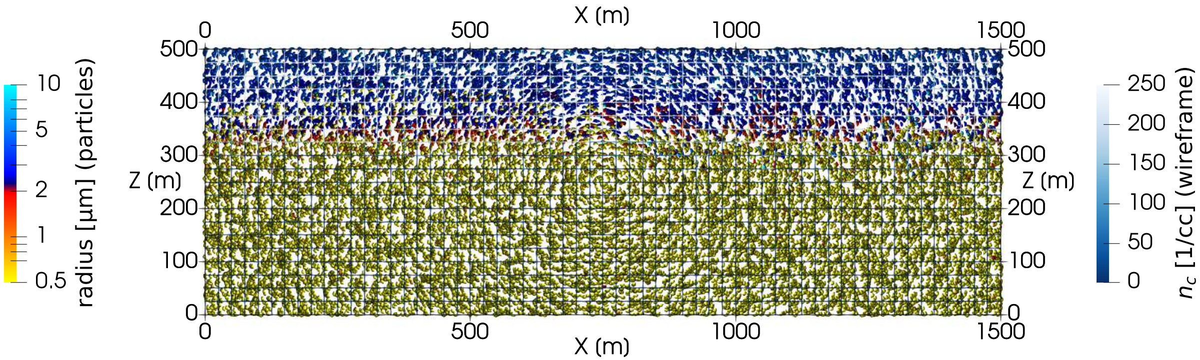

16+16 super-particles/cell for INP-rich + INP-free particles

$N_{\text{aer}} = 300/cc$ (two-mode lognormal) $N_{\text{INP}} = 150/L$ (lognormal, $D_g = 0.74$ μm, $\sigma_g = 2.55$)

spin-up = freezing off; subsequently frozen particles act as tracers

Time: 330 s (spin-up till 600.0 s)

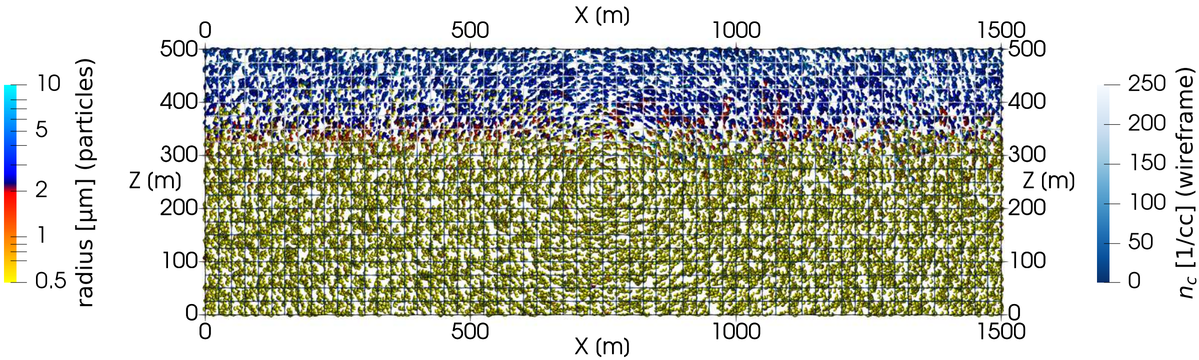

16+16 super-particles/cell for INP-rich + INP-free particles

$N_{aer} = 300/cc$ (two-mode lognormal) $N_{INP} = 150/L$ (lognormal, $D_g = 0.74$ μm, $\sigma_g = 2.55$)

spin-up = freezing off; subsequently frozen particles act as tracers

Time: 360 s (spin-up till 600.0 s)

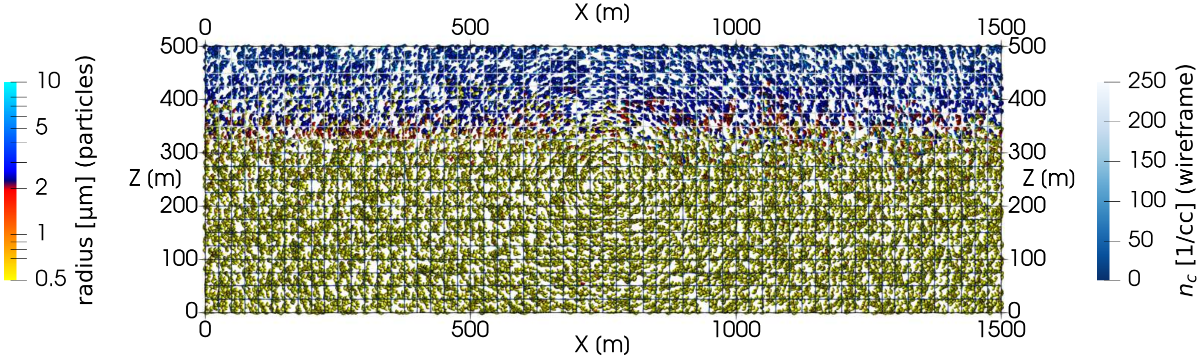

16+16 super-particles/cell for INP-rich + INP-free particles
$N_{aer} = 300/cc$ (two-mode lognormal) $N_{INP} = 150/L$ (lognormal, $D_g = 0.74$ µm, $\sigma_g = 2.55$)
spin-up = freezing off; subsequently frozen particles act as tracers

Time: 390 s (spin-up till 600.0 s)

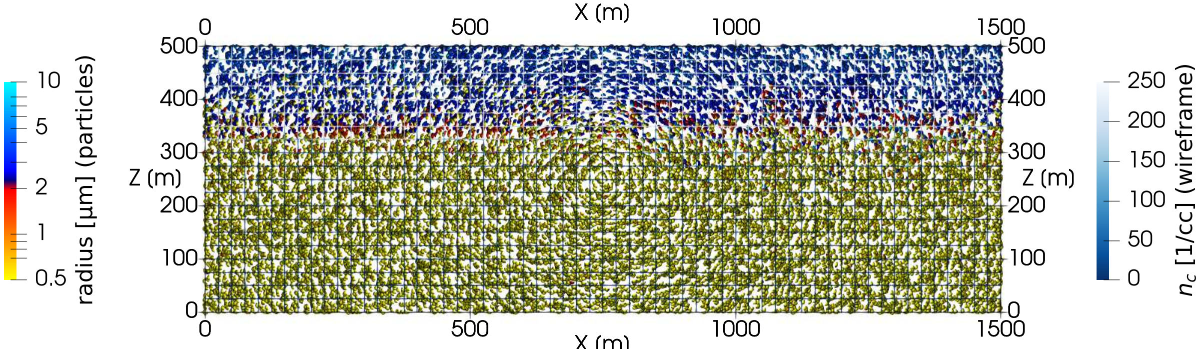

16+16 super-particles/cell for INP-rich + INP-free particles

$N_{\text{aer}} = 300/cc$ (two-mode lognormal) $N_{\text{INP}} = 150/L$ (lognormal, $D_g = 0.74$ μm, $\sigma_g = 2.55$)

spin-up = freezing off; subsequently frozen particles act as tracers

Time: 420 s (spin-up till 600.0 s)

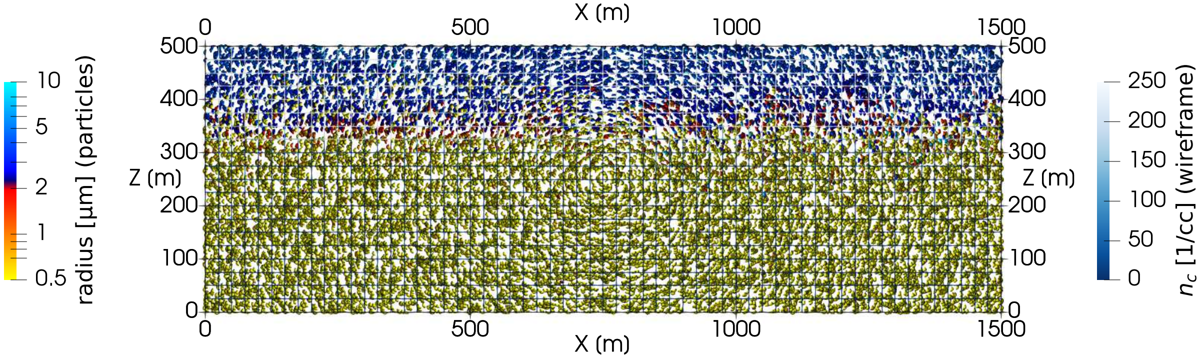

16+16 super-particles/cell for INP-rich + INP-free particles

$N_{aer} = 300/cc$ (two-mode lognormal) $N_{INP} = 150/L$ (lognormal, $D_g = 0.74$ μm, $\sigma_g = 2.55$)

spin-up = freezing off; subsequently frozen particles act as tracers

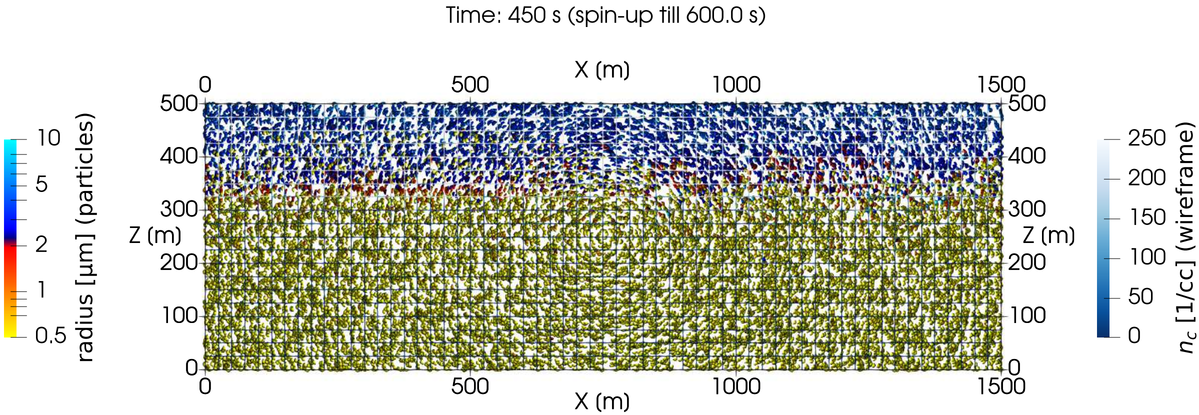

16+16 super-particles/cell for INP-rich + INP-free particles

$N_{\text{aer}} = 300/cc$ (two-mode lognormal) $N_{\text{INP}} = 150/L$ (lognormal, $D_g = 0.74$ μm, $\sigma_g = 2.55$)

spin-up = freezing off; subsequently frozen particles act as tracers

Time: 480 s (spin-up till 600.0 s)

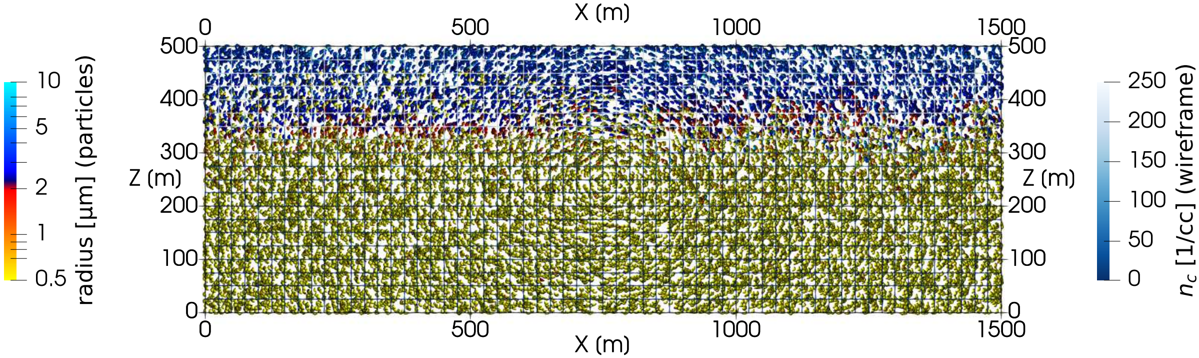

16+16 super-particles/cell for INP-rich + INP-free particles

$N_{\text{aer}} = 300/cc$ (two-mode lognormal) $N_{\text{INP}} = 150/L$ (lognormal, $D_g = 0.74$ μm, $\sigma_g = 2.55$)

spin-up = freezing off; subsequently frozen particles act as tracers

Time: 510 s (spin-up till 600.0 s)

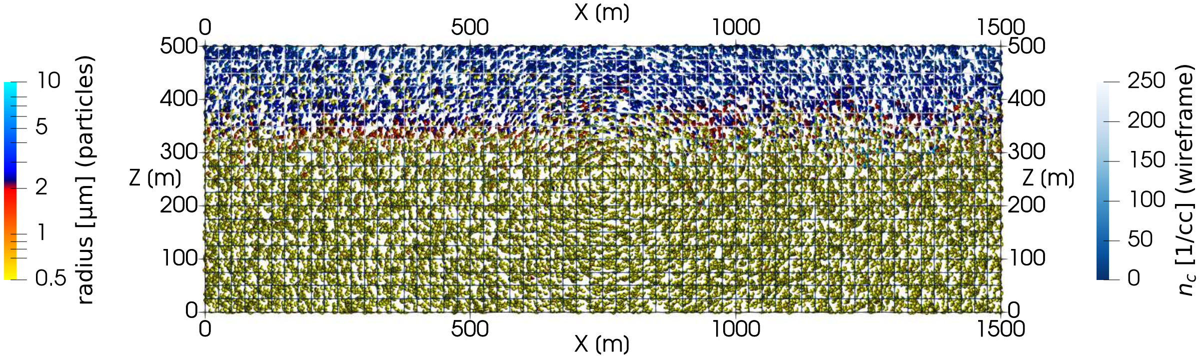

16+16 super-particles/cell for INP-rich + INP-free particles

$N_{aer} = 300/cc$ (two-mode lognormal) $N_{INP} = 150/L$ (lognormal, $D_g = 0.74$ μm, $\sigma_g = 2.55$)

spin-up = freezing off; subsequently frozen particles act as tracers

Time: 540 s (spin-up till 600.0 s)

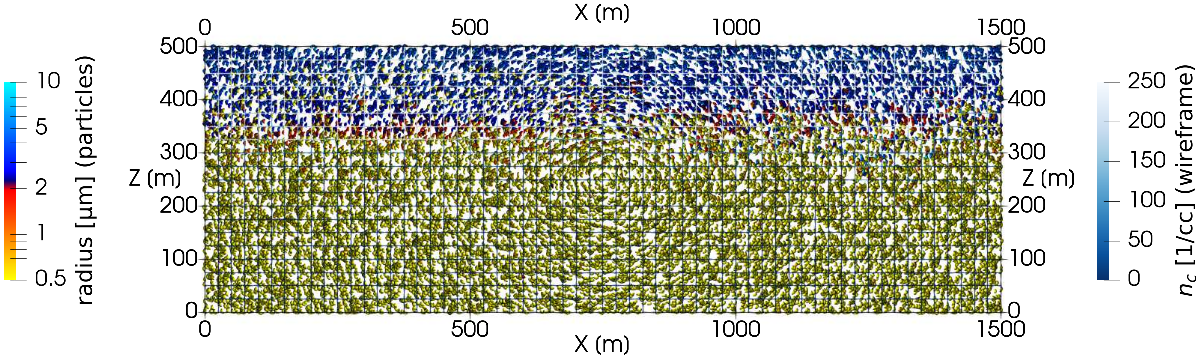

16+16 super-particles/cell for INP-rich + INP-free particles

$N_{\mathrm{aer}} = 300/cc$ (two-mode lognormal) $N_{\mathrm{INP}} = 150/L$ (lognormal, $D_g = 0.74$ µm, $\sigma_g = 2.55$)

spin-up = freezing off; subsequently frozen particles act as tracers

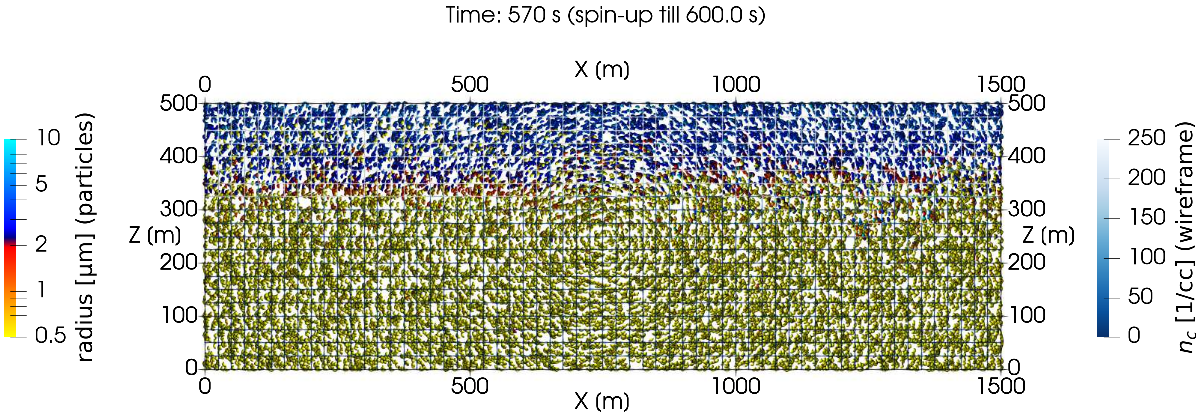

16+16 super-particles/cell for INP-rich + INP-free particles

$N_{\rm aer}$ = 300/cc (two-mode lognormal) $N_{\rm INP}$ = 150/L (lognormal, D_g = 0.74 μm, σ_g = 2.55)

spin-up = freezing off; subsequently frozen particles act as tracers

Time: 600 s (spin-up till 600.0 s)

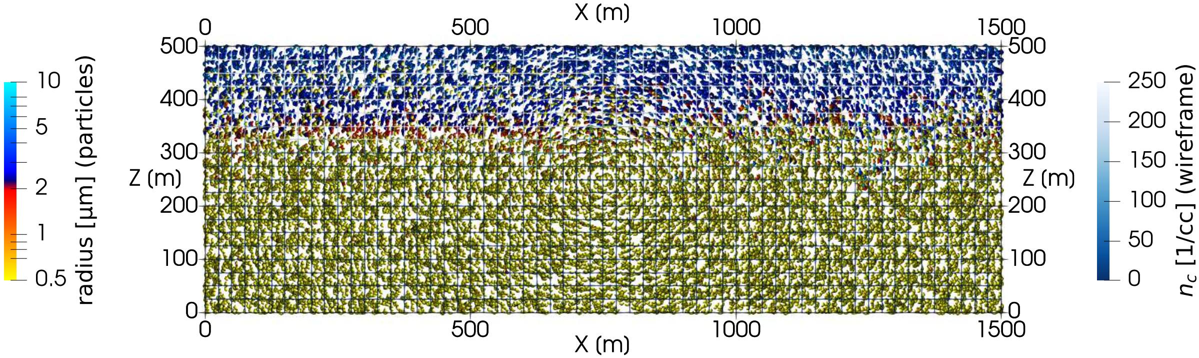

16+16 super-particles/cell for INP-rich + INP-free particles

$N_{aer} = 300/cc$ (two-mode lognormal) $N_{INP} = 150/L$ (lognormal, $D_g = 0.74$ µm, $\sigma_g = 2.55$)

spin-up = freezing off; subsequently frozen particles act as tracers

Time: 630 s (spin-up till 600.0 s)

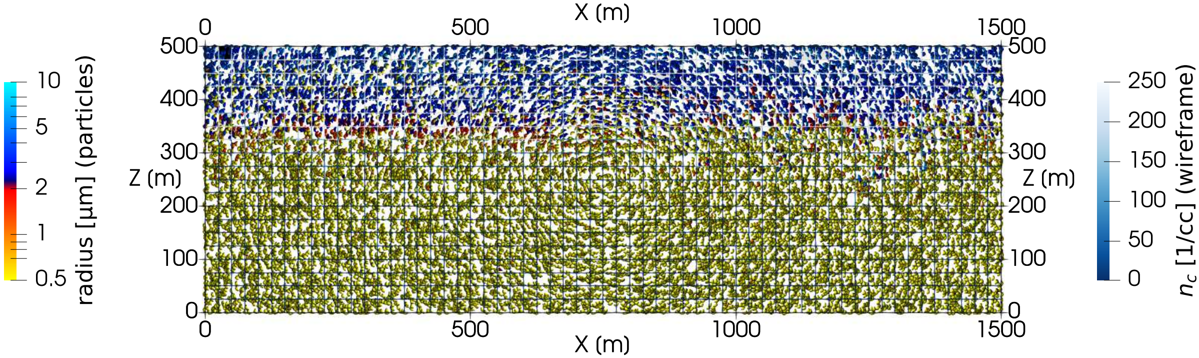

16+16 super-particles/cell for INP-rich + INP-free particles
$N_{\text{aer}} = 300/cc$ (two-mode lognormal) $N_{\text{INP}} = 150/L$ (lognormal, $D_g = 0.74$ μm, $\sigma_g = 2.55$)
spin-up = freezing off; subsequently frozen particles act as tracers

Time: 660 s (spin-up till 600.0 s)

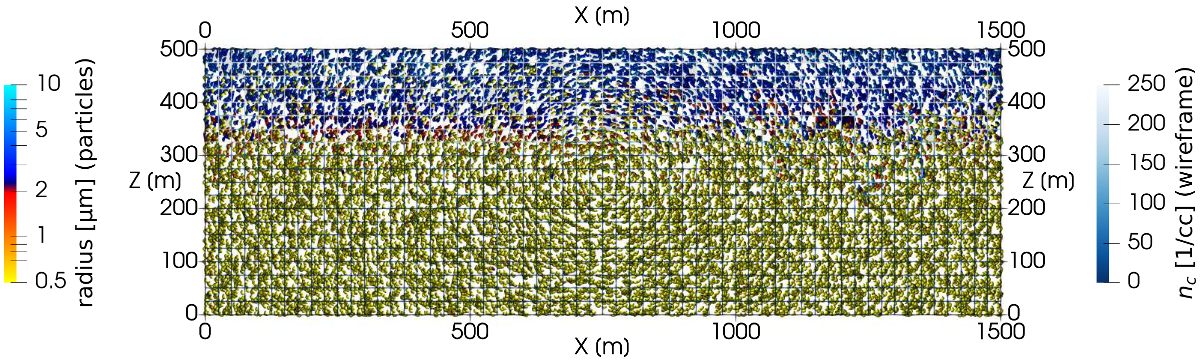

16+16 super-particles/cell for INP-rich + INP-free particles

$N_{\text{aer}} = 300/cc$ (two-mode lognormal) $N_{\text{INP}} = 150/L$ (lognormal, $D_g = 0.74$ μm, $\sigma_g = 2.55$)

spin-up = freezing off; subsequently frozen particles act as tracers

Time: 690 s (spin-up till 600.0 s)

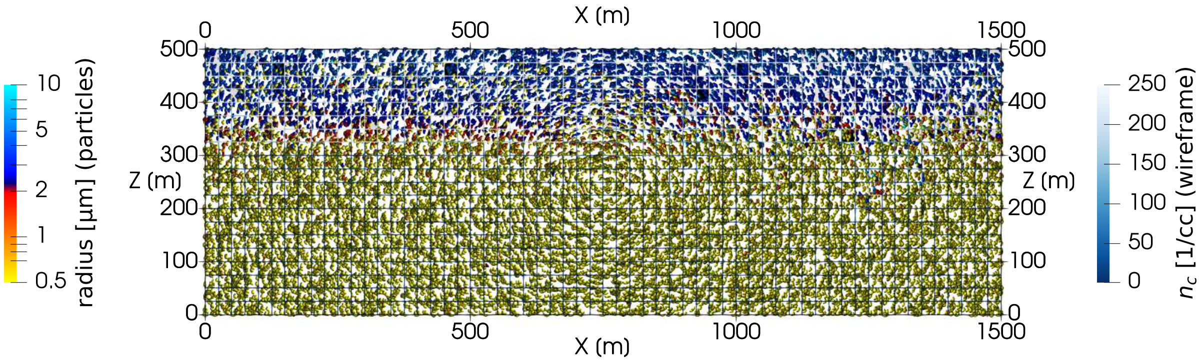

16+16 super-particles/cell for INP-rich + INP-free particles

$N_{\text{aer}} = 300/cc$ (two-mode lognormal) $N_{\text{INP}} = 150/L$ (lognormal, $D_g = 0.74$ µm, $\sigma_g = 2.55$)

spin-up = freezing off; subsequently frozen particles act as tracers

Time: 720 s (spin-up till 600.0 s)

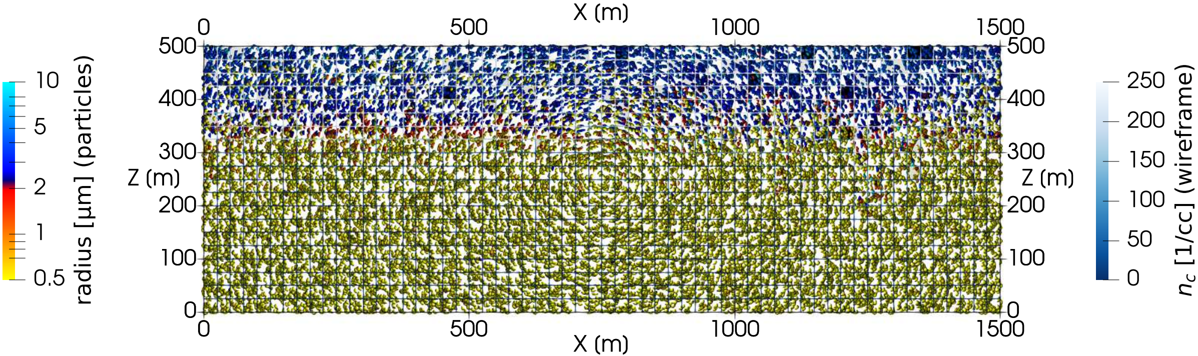

16+16 super-particles/cell for INP-rich + INP-free particles

$N_{aer} = 300/cc$ (two-mode lognormal) $N_{INP} = 150/L$ (lognormal, $D_g = 0.74$ μm, $\sigma_g = 2.55$)

spin-up = freezing off; subsequently frozen particles act as tracers

Time: 750 s (spin-up till 600.0 s)

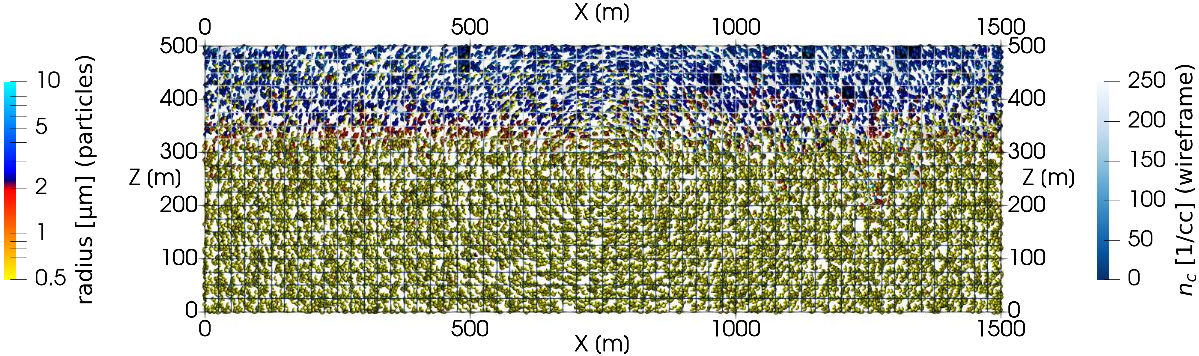

16+16 super-particles/cell for INP-rich + INP-free particles

$N_{aer} = 300/cc$ (two-mode lognormal) $N_{INP} = 150/L$ (lognormal, $D_g = 0.74$ μm, $\sigma_g = 2.55$)

spin-up = freezing off; subsequently frozen particles act as tracers

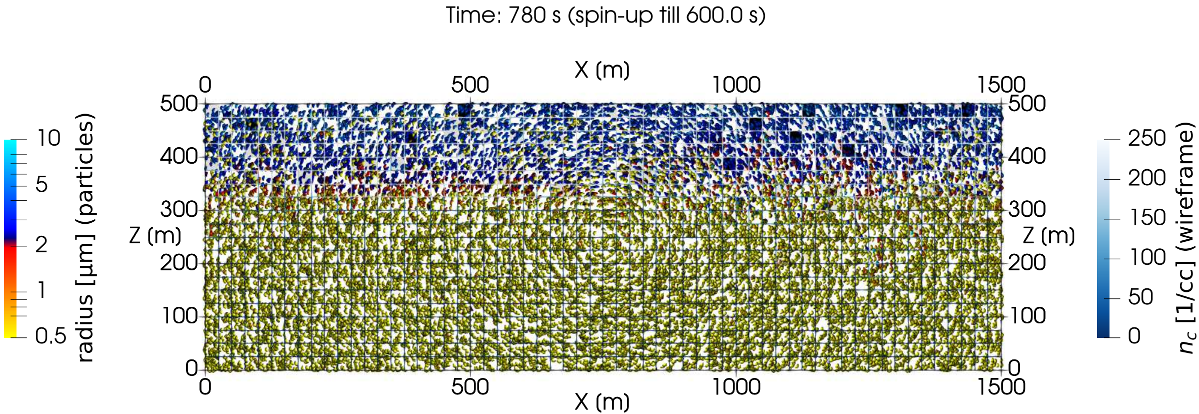

16+16 super-particles/cell for INP-rich + INP-free particles

$N_{aer} = 300/cc$ (two-mode lognormal) $N_{INP} = 150/L$ (lognormal, $D_g = 0.74$ µm, $\sigma_g = 2.55$)

spin-up = freezing off; subsequently frozen particles act as tracers

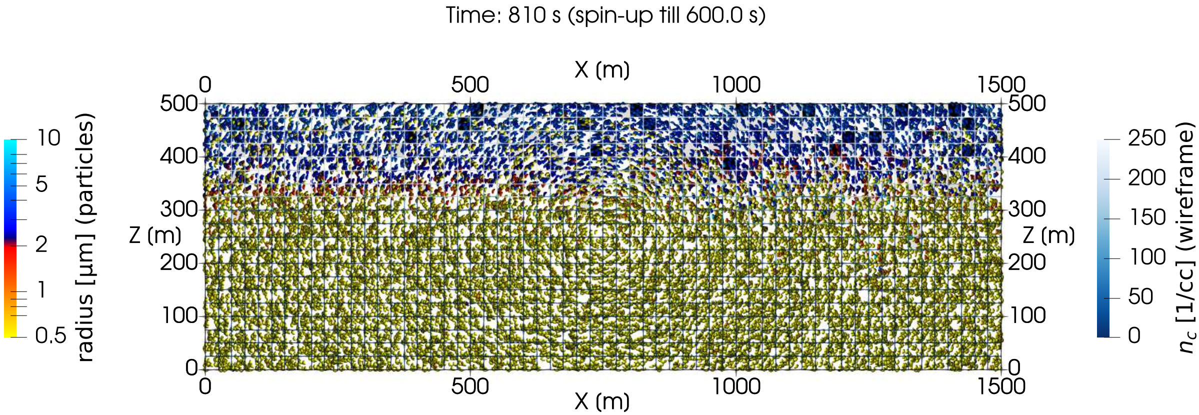

16+16 super-particles/cell for INP-rich + INP-free particles

$N_{\text{aer}} = 300/cc$ (two-mode lognormal) $N_{\text{INP}} = 150/L$ (lognormal, $D_g = 0.74$ µm, $\sigma_g = 2.55$)

spin-up = freezing off; subsequently frozen particles act as tracers

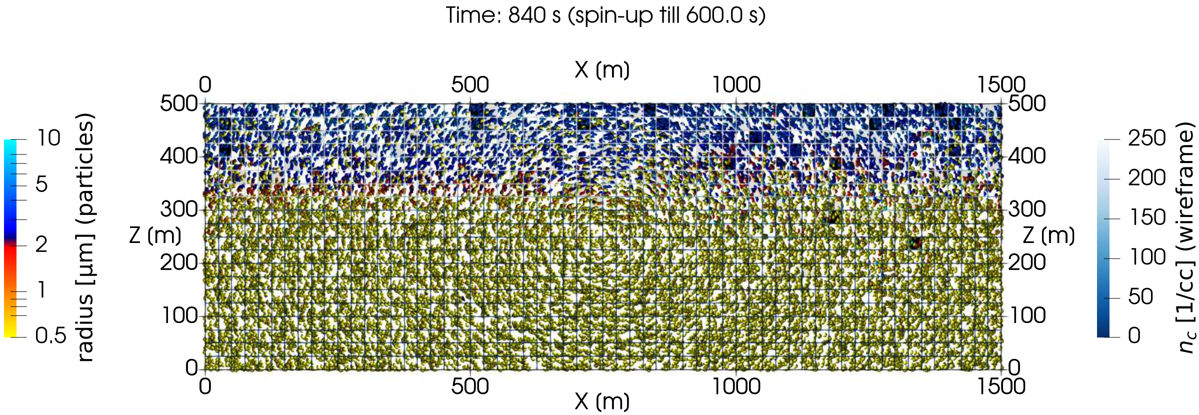

16+16 super-particles/cell for INP-rich + INP-free particles
$N_{aer} = 300/cc$ (two-mode lognormal) $N_{INP} = 150/L$ (lognormal, $D_g = 0.74$ µm, $\sigma_g = 2.55$)
spin-up = freezing off; subsequently frozen particles act as tracers

Time: 870 s (spin-up till 600.0 s)

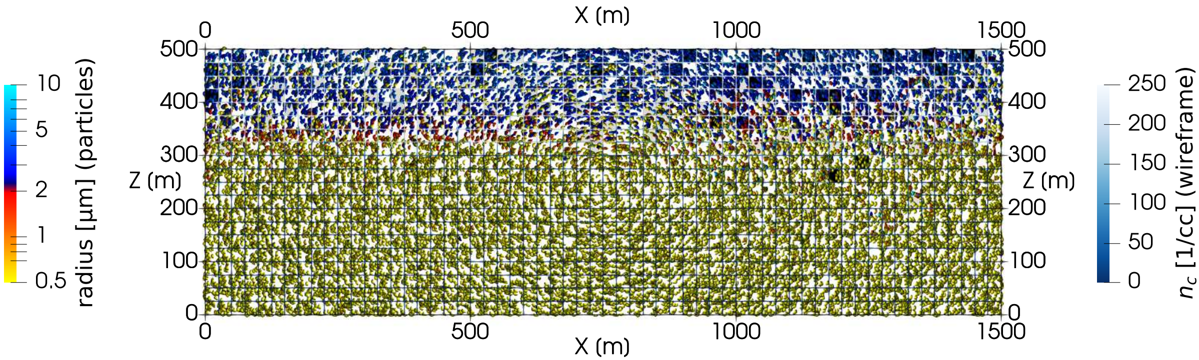

16+16 super-particles/cell for INP-rich + INP-free particles

$N_{aer} = 300/cc$ (two-mode lognormal) $N_{INP} = 150/L$ (lognormal, $D_g = 0.74$ μm, $\sigma_g = 2.55$)

spin-up = freezing off; subsequently frozen particles act as tracers

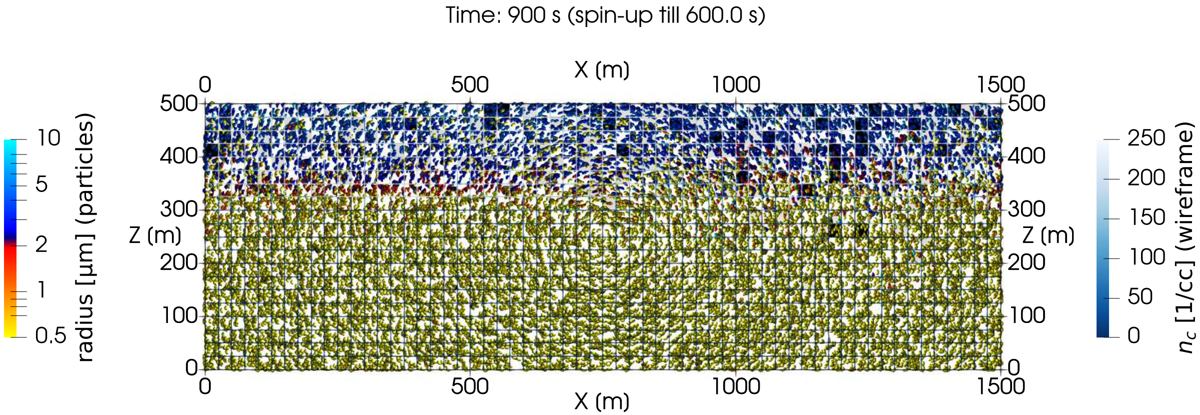

16+16 super-particles/cell for INP-rich + INP-free particles

$N_{aer} = 300/cc$ (two-mode lognormal) $N_{INP} = 150/L$ (lognormal, $D_g = 0.74$ µm, $\sigma_g = 2.55$)

spin-up = freezing off; subsequently frozen particles act as tracers

Time: 930 s (spin-up till 600.0 s)

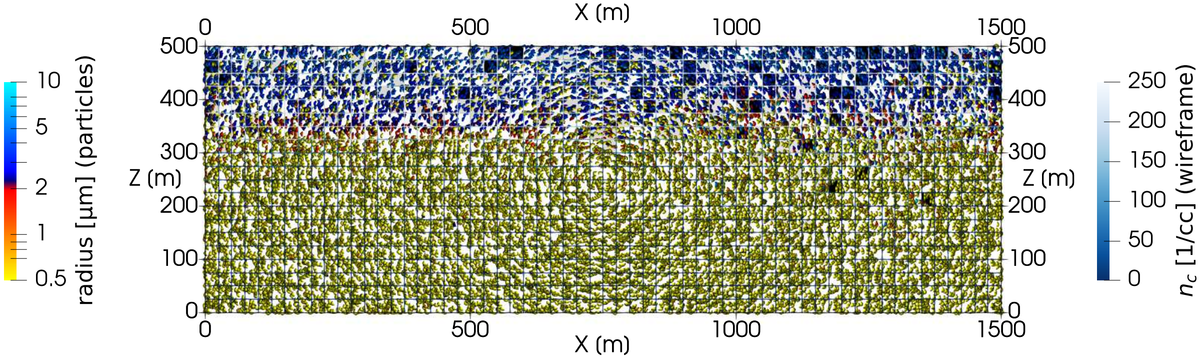

16+16 super-particles/cell for INP-rich + INP-free particles
$N_{aer} = 300/cc$ (two-mode lognormal) $N_{INP} = 150/L$ (lognormal, $D_g = 0.74$ µm, $\sigma_g = 2.55$)
spin-up = freezing off; subsequently frozen particles act as tracers

Time: 960 s (spin-up till 600.0 s)

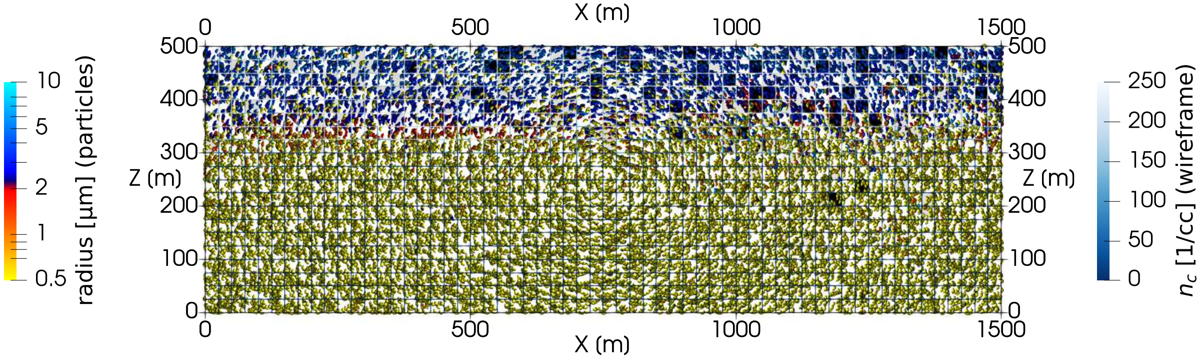

16+16 super-particles/cell for INP-rich + INP-free particles

$N_{aer} = 300/cc$ (two-mode lognormal) $N_{INP} = 150/L$ (lognormal, $D_g = 0.74$ µm, $\sigma_g = 2.55$)

spin-up = freezing off; subsequently frozen particles act as tracers

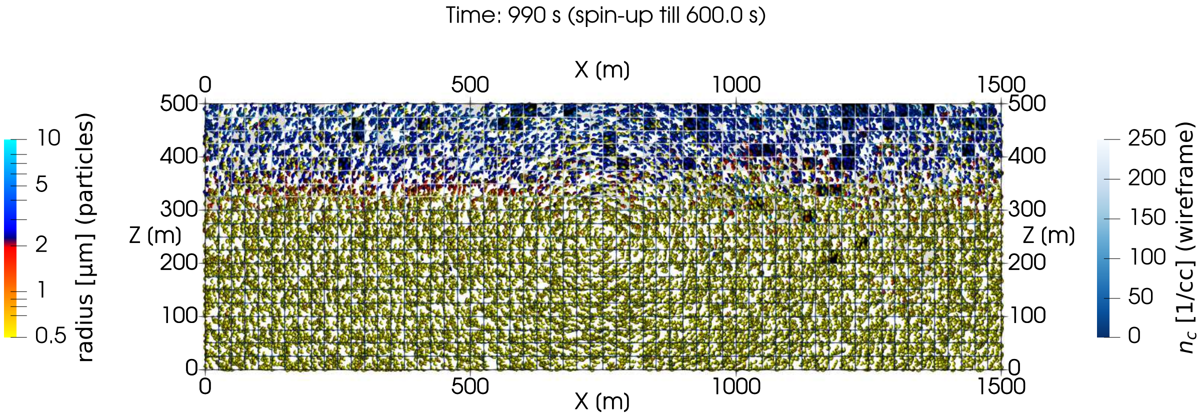

16+16 super-particles/cell for INP-rich + INP-free particles

$N_{aer} = 300/cc$ (two-mode lognormal) $N_{INP} = 150/L$ (lognormal, $D_g = 0.74$ μm, $\sigma_g = 2.55$)

spin-up = freezing off; subsequently frozen particles act as tracers

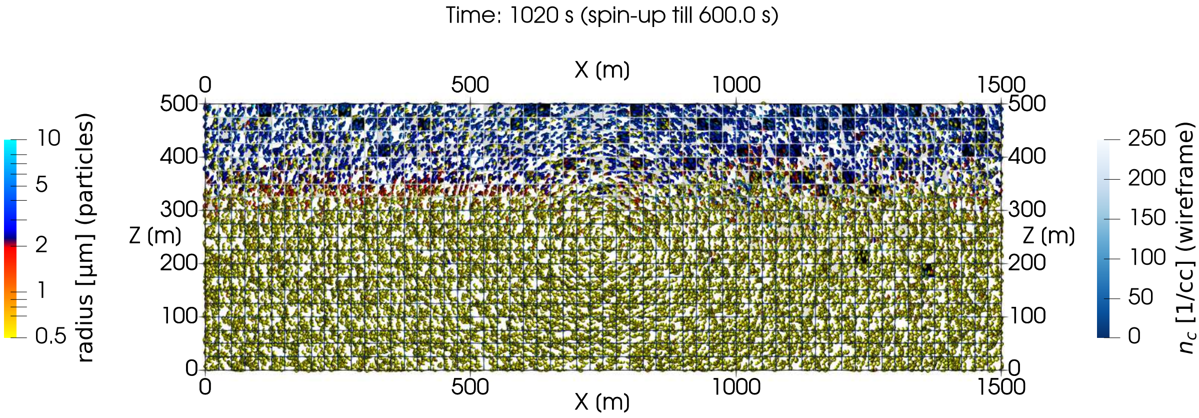

16+16 super-particles/cell for INP-rich + INP-free particles
$N_{\text{aer}} = 300/cc$ (two-mode lognormal) $N_{\text{INP}} = 150/L$ (lognormal, $D_g = 0.74$ µm, $\sigma_g = 2.55$)
spin-up = freezing off; subsequently frozen particles act as tracers

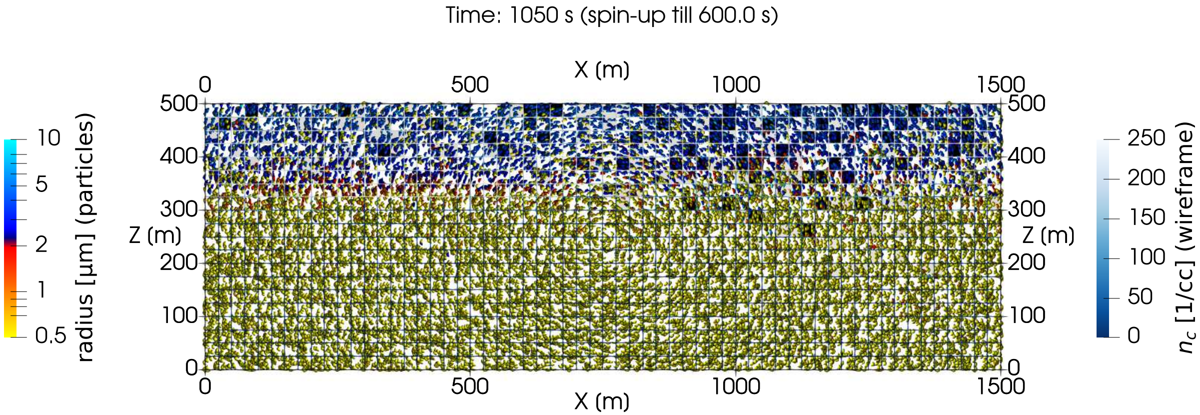

16+16 super-particles/cell for INP-rich + INP-free particles
$N_{\text{aer}} = 300/cc$ (two-mode lognormal) $N_{\text{INP}} = 150/L$ (lognormal, $D_g = 0.74$ μm, $\sigma_g = 2.55$)
spin-up = freezing off; subsequently frozen particles act as tracers

Time: 1080 s (spin-up till 600.0 s)

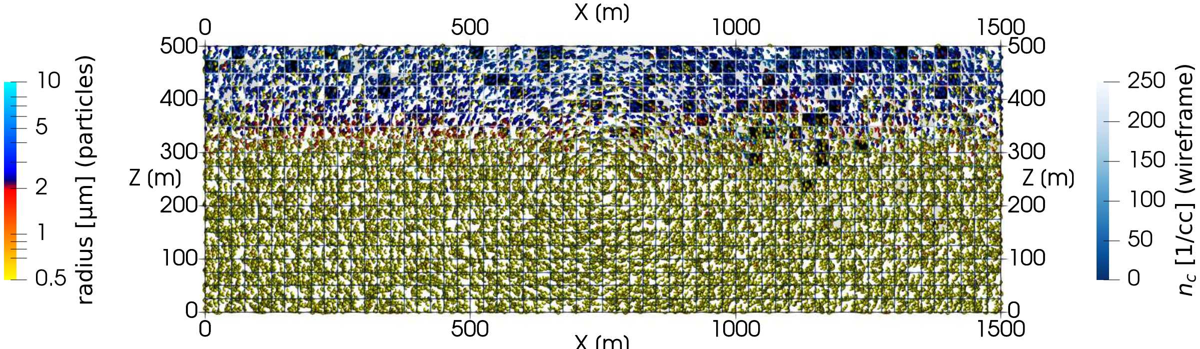

16+16 super-particles/cell for INP-rich + INP-free particles

$N_{aer} = 300/cc$ (two-mode lognormal) $N_{INP} = 150/L$ (lognormal, $D_g = 0.74$ µm, $\sigma_g = 2.55$)

spin-up = freezing off; subsequently frozen particles act as tracers

Time: 1110 s (spin-up till 600.0 s)

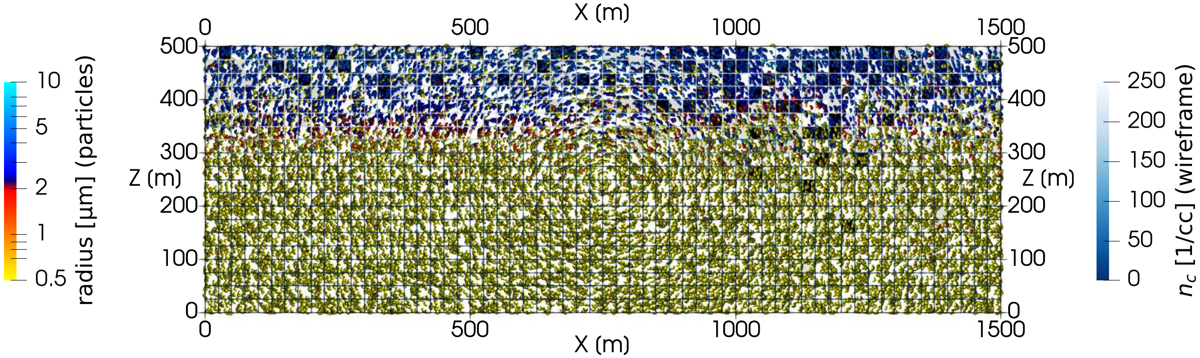

16+16 super-particles/cell for INP-rich + INP-free particles

$N_{aer} = 300/cc$ (two-mode lognormal) $N_{INP} = 150/L$ (lognormal, $D_g = 0.74$ μm, $\sigma_g = 2.55$)

spin-up = freezing off; subsequently frozen particles act as tracers

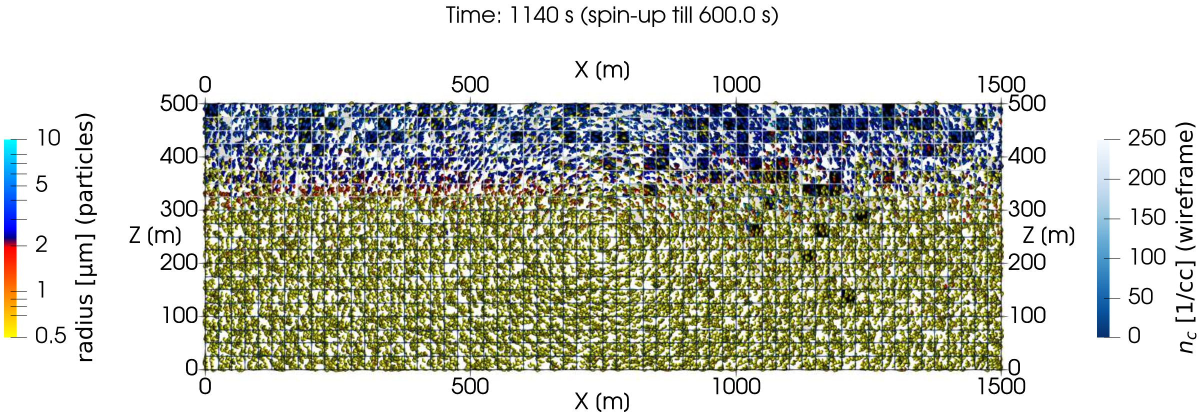

16+16 super-particles/cell for INP-rich + INP-free particles
$N_{aer} = 300/cc$ (two-mode lognormal) $N_{INP} = 150/L$ (lognormal, $D_g = 0.74$ μm, $\sigma_g = 2.55$)
spin-up = freezing off; subsequently frozen particles act as tracers

Time: 1170 s (spin-up till 600.0 s)

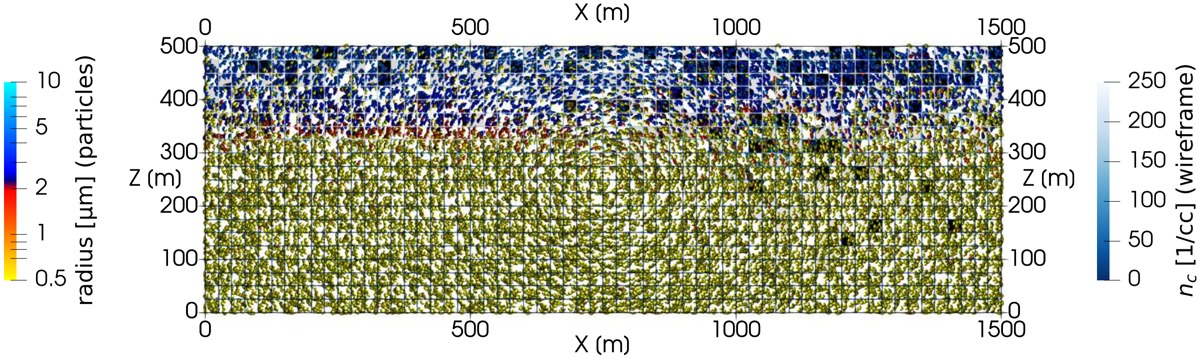

16+16 super-particles/cell for INP-rich + INP-free particles

$N_{aer} = 300/cc$ (two-mode lognormal) $N_{INP} = 150/L$ (lognormal, $D_g = 0.74$ μm, $\sigma_g = 2.55$)

spin-up = freezing off; subsequently frozen particles act as tracers

Time: 1200 s (spin-up till 600.0 s)

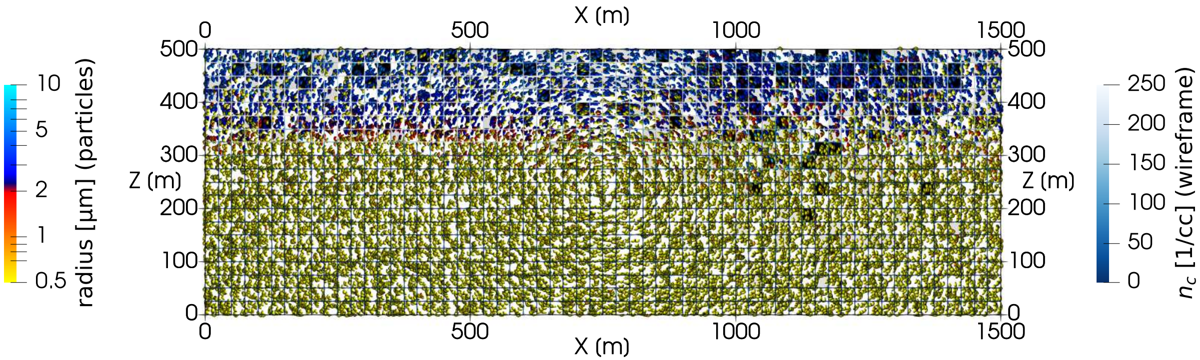

16+16 super-particles/cell for INP-rich + INP-free particles

$N_{\text{aer}} = 300/cc$ (two-mode lognormal) $N_{\text{INP}} = 150/L$ (lognormal, $D_g = 0.74$ μm, $\sigma_g = 2.55$)

spin-up = freezing off; subsequently frozen particles act as tracers

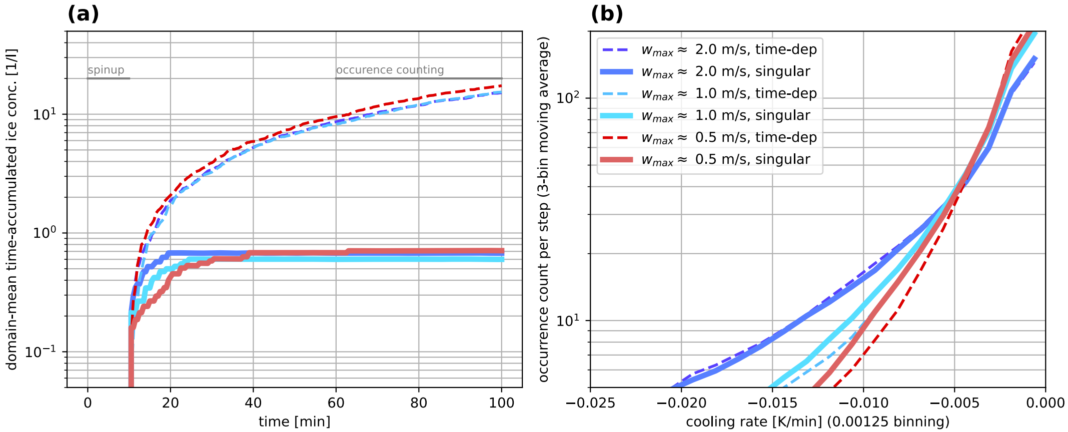

- singular vs. time-dependent markedly different (consistent with box model for $c \ll 1K/min$)

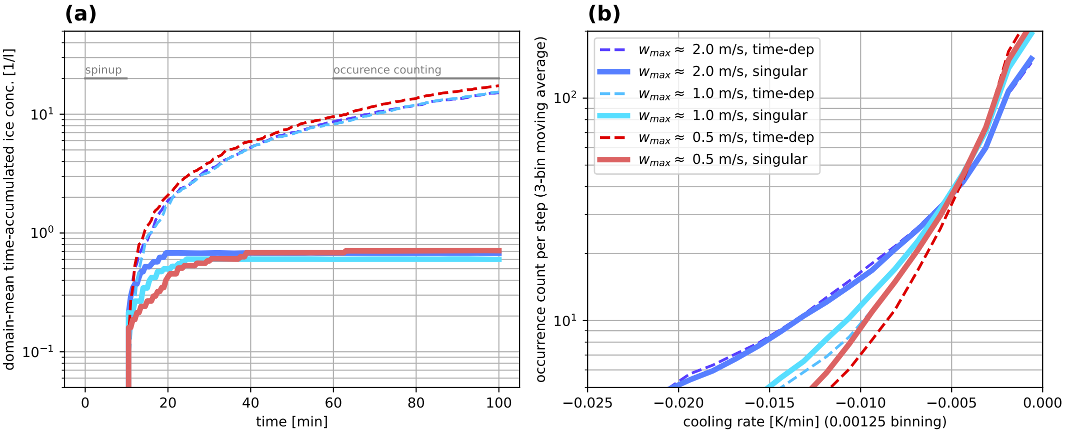

- singular vs. time-dependent markedly different (consistent with box model for $c \ll 1K/min$)
- range of cooling rates in simple flow (far from $c \sim 1$ K/min for AIDA as in Niemand et al. 2012)

Opinion: Cloud-phase climate feedback and the importance of ice-nucleating particles

Benjamin J. Murray[1], Kenneth S. Carslaw[1], and Paul R. Field[1,2]

Atmospheric Chemistry and Physics
Atmos. Chem. Phys., 21, 665–679, 2021
https://doi.org/10.5194/acp-21-665-2021

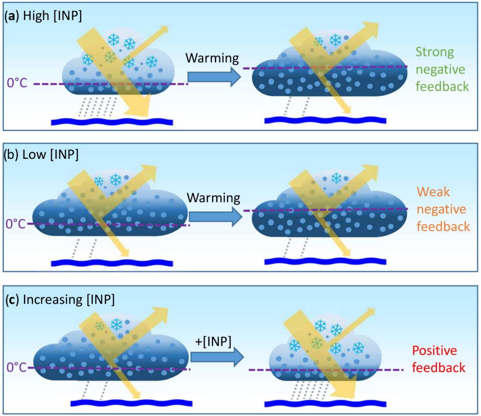

- *"it is becoming very clear that the cloud-phase feedback contributes substantially to the uncertainty in predictions of the rate at which our planet will warm in response to CO_2 emissions"*

Opinion: Cloud-phase climate feedback and the importance of ice-nucleating particles

Benjamin J. Murray[1], Kenneth S. Carslaw[1], and Paul R. Field[1,2]

Atmospheric Chemistry and Physics
Atmos. Chem. Phys., 21, 665–679, 2021
https://doi.org/10.5194/acp-21-665-2021

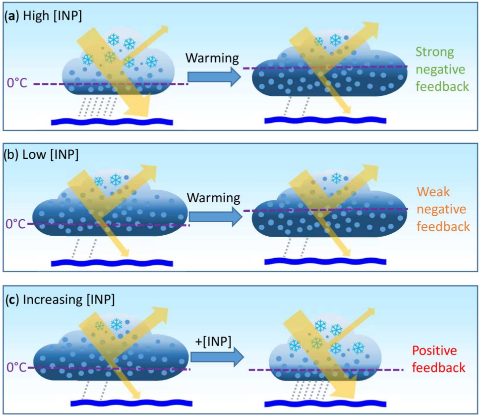

- *"it is becoming very clear that the cloud-phase feedback contributes substantially to the uncertainty in predictions of the rate at which our planet will warm in response to CO_2 emissions"*
- *"core physical process that drives the cloud-phase feedback is the transition to clouds with more liquid water and less ice as the isotherms shift upwards in a warmer world"*

Opinion: Cloud-phase climate feedback and the importance of ice-nucleating particles

Benjamin J. Murray[1], Kenneth S. Carslaw[1], and Paul R. Field[1,2]

Atmospheric Chemistry and Physics
Atmos. Chem. Phys., 21, 665–679, 2021
https://doi.org/10.5194/acp-21-665-2021

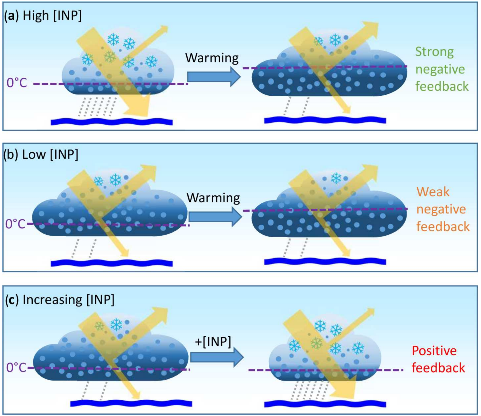

- *"it is becoming very clear that the cloud-phase feedback contributes substantially to the uncertainty in predictions of the rate at which our planet will warm in response to CO_2 emissions"*
- *"core physical process that drives the cloud-phase feedback is the transition to clouds with more liquid water and less ice as the isotherms shift upwards in a warmer world"*
- *"models need to improve their representation of ice-related microphysical processes; in particular, they need to include a direct link to aerosol type, specifically INPs"*

Opinion: Cloud-phase climate feedback and the importance of ice-nucleating particles

Benjamin J. Murray[1], Kenneth S. Carslaw[1], and Paul R. Field[1,2]

Atmospheric Chemistry and Physics Open Access EGU
Atmos. Chem. Phys., 21, 665–679, 2021
https://doi.org/10.5194/acp-21-665-2021

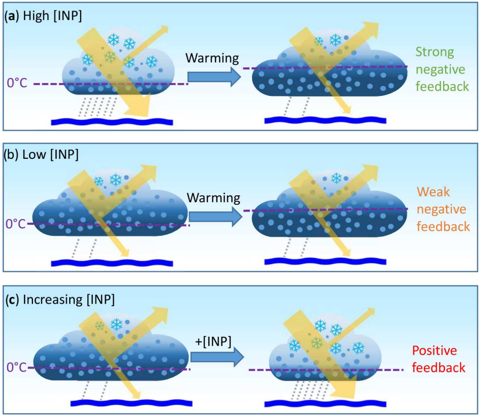

- *"it is becoming very clear that the cloud-phase feedback contributes substantially to the uncertainty in predictions of the rate at which our planet will warm in response to CO_2 emissions"*
- *"core physical process that drives the cloud-phase feedback is the transition to clouds with more liquid water and less ice as the isotherms shift upwards in a warmer world"*
- *"models need to improve their representation of ice-related microphysical processes; in particular, they need to include a direct link to aerosol type, specifically INPs"*
- *"must also represent the INP removal processes, which in turn depend on a correct representation of the microphysics"*

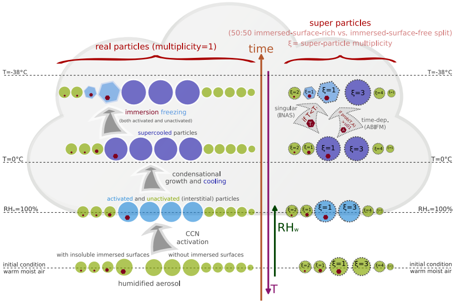

super particles
(50:50 immersed-surface-rich vs. immersed-surface-free split)
ξ = super-particle multiplicity
real particles (multiplicity=1)
time
T=-38°C
immersion freezing
(both activated and unactivated)
singular
(INAS)
time-dep.
(ABIFM)
supercooled particles
T=0°C
condensational
growth and cooling
activated and unactivated (interstitial) particles
RHw=100%
RHw
CCN
activation
with insoluble immersed surfaces
without immersed surfaces
initial condition
warm moist air
humidified aerosol
T

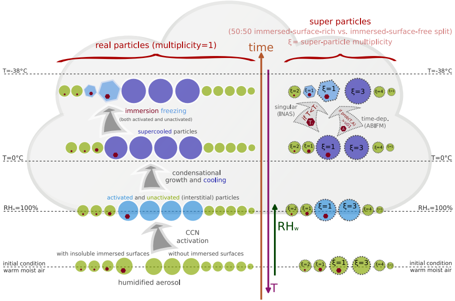

super particles
(50:50 immersed-surface-rich vs. immersed-surface-free split)
ξ = super-particle multiplicity
real particles (multiplicity=1)
time
T=-38°C
immersion freezing
(both activated and unactivated)
supercooled particles
singular
(INAS)
time-dep.
(ABIFM)
T=0°C
condensational
growth and cooling
activated and unactivated (interstitial) particles
RHw=100%
RHw
CCN
activation
with insoluble immersed surfaces
without immersed surfaces
initial condition
warm moist air
humidified aerosol
T

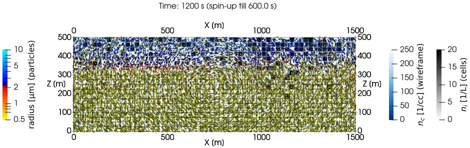

Time: 1200 s (spin-up till 600.0 s)
X (m)
Z (m)
radius [μm] (particles)
n_c [1/cc] (wireframe)
n_i [1/L] (cells)

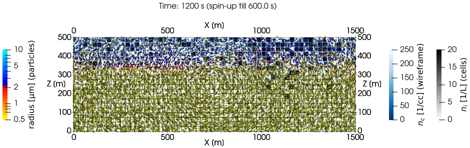

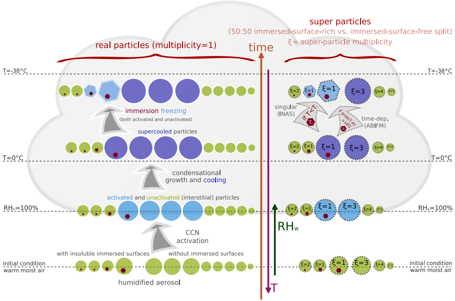

PySDM 2.20

```
pip install PySDM
```

Research topics offered by the AGH Doctoral School in the academic year 2023/2024

If you wish to find research topics related to the area of your interest, type a few keywords into the search box and click the Search button. The general search explores complete topic descriptions and returns topics that contain all the provided words. If you want to limit your search to some of the table columns use the search boxes below the corresponding column labels. You can also sort the data by clicking the table headers.

Search for: microphysics Search Clear filter

Topic ID	Research topic	Faculty	Supervisor	Leading discipline	Funding source
1202	Modelling of isotopic signatures in precipitation using particle-based cloud microphysics	Faculty of Physics and Applied Computer Science	dr hab. inż. Mirosław Zimnoch	physical sciences	Subsidy

Research topics offered by the AGH Doctoral School in the academic year 2023/2024

If you wish to find research topics related to the area of your interest, type a few keywords into the search box and click the Search button. The general search explores complete topic descriptions and returns topics that contain all the provided words. If you want to limit your search to some of the table columns use the search boxes below the corresponding column labels. You can also sort the data by clicking the table headers.

Search for: microphysics | Search | Clear filter

Topic ID	Research topic	Faculty	Supervisor	Leading discipline	Funding source
1202	Modelling of isotopic signatures in precipitation using particle-based cloud microphysics	Faculty of Physics and Applied Computer Science	dr hab. inż. Mirosław Zimnoch	physical sciences	Subsidy

ASR Atmospheric System Research
DOE ASR grant no. DE-SC0021034

Research topics offered by the AGH Doctoral School in the academic year 2023/2024

If you wish to find research topics related to the area of your interest, type a few keywords into the search box and click the Search button. The general search explores complete topic descriptions and returns topics that contain all the provided words. If you want to limit your search to some of the table columns use the search boxes below the corresponding column labels. You can also sort the data by clicking the table headers.

Search for: microphysics [Search] [Clear filter]

Topic ID	Research topic	Faculty	Supervisor	Leading discipline	Funding source
1202	Modelling of isotopic signatures in precipitation using particle-based cloud microphysics	Faculty of Physics and Applied Computer Science	dr hab. inż. Mirosław Zimnoch	physical sciences	Subsidy

ASR Atmospheric System Research
DOE ASR grant no. DE-SC0021034

NCN grant no. 2020/39/D/ST10/01220

Research topics offered by the AGH Doctoral School in the academic year 2023/2024

If you wish to find research topics related to the area of your interest, type a few keywords into the search box and click the Search button. The general search explores complete topic descriptions and returns topics that contain all the provided words. If you want to limit your search to some of the table columns use the search boxes below the corresponding column labels. You can also sort the data by clicking the table headers.

Search for: microphysics | Search | Clear filter

Topic ID	Research topic	Faculty	Supervisor	Leading discipline	Funding source
1202	Modelling of isotopic signatures in precipitation using particle-based cloud microphysics	Faculty of Physics and Applied Computer Science	dr hab. inż. Mirosław Zimnoch	physical sciences	Subsidy

ASR Atmospheric System Research — DOE ASR grant no. DE-SC0021034
NCN grant no. 2020/39/D/ST10/01220
python™ /open-atmos

Szkoła Doktorska AGH

Akademia Górniczo-Hutnicza im. Stanisława Staszica w Krakowie

Research topics offered by the AGH Doctoral School in the academic year 2023/2024

If you wish to find research topics related to the area of your interest, type a few keywords into the search box and click the Search button. The general search explores complete topic descriptions and returns topics that contain all the provided words. If you want to limit your search to some of the table columns use the search boxes below the corresponding column labels. You can also sort the data by clicking the table headers.

Search for: microphysics Search Clear filter

Topic ID	Research topic	Faculty	Supervisor	Leading discipline	Funding source
1202	Modelling of isotopic signatures in precipitation using particle-based cloud microphysics	Faculty of Physics and Applied Computer Science	dr hab. inż. Mirosław Zimnoch	physical sciences	Subsidy

ASR Atmospheric System Research DOE ASR grant no. DE-SC0021034

NCN grant no. 2020/39/D/ST10/01220

python /open-atmos

Dziękuję za uwagę!